Journal of Materials Chemistry A

ROYAL SOCIETY OF CHEMISTRY

REVIEW

View Article Online
View Journal | View Issue

Cite this: J. Mater. Chem. A, 2024, 12, 23147

Enhancing electrochemical performance and corrosion resistance of nickel-based catalysts in seawater electrolysis: focusing on OER and HER

Yuemin Xin,[a] Qianqian Hua,[a] Chengjie Li,*[b] Haiding Zhu,[c] Liguo Gao,[a] Xuefeng Ren,*[a] Peixia Yang*[d] and Anmin Liu*[a]

Hydrogen production by electrochemical hydrogen evolution reaction (HER) using eco-friendly seawater electrolysis can help address the energy shortage. However, insoluble precipitates form from elements of magnesium, calcium, and chlorine ions with the oxygen evolution reaction (OER) will cause electrode degradation. Currently, commercially viable catalysts are mostly comprised of precious metal Pt-based catalysts, which are expensive and limited in availability. The critical factor for hydrogen production from seawater electrolysis is the development of highly efficient and corrosion-resistant catalysts. Nickel-based electrocatalysts, which are cost-effective with conductivity and corrosion resistance, are a prospective substitute for precious metal catalysts. This review summarizes contemporary methods and ideas for improving the performance of nickel-based electrocatalysts and stability for HER and OER in seawater, focusing on strengthening electrochemical performance and corrosion resistance. It is a comprehensive resource for advancing nickel-based electrocatalysts in seawater electrolysis, guiding the development of more efficient electrocatalysts and bolstering long-term reliability and stability in seawater environments.

Received 16th May 2024
Accepted 3rd July 2024

DOI: 10.1039/d4ta03393k

rsc.li/materials-a

1. Introduction

In the 21st century, humankind has faced increasingly severe energy crises and environmental problems such as global warming.[1,2] These challenges have prompted a search for new energy sources to replace traditional fossil fuels, making carbon neutrality the mainstream direction for international development.[3] At the recent *28th Conference of the Parties to the United Nations Framework Convention on Climate Change*, UNFCCC (COP28) climate summit in Dubai, 190 countries agreed to move away from fossil fuel dependence, signaling the end of the fossil fuel era and growing demand for renewable energy.[4–6] Hydrogen energy, with its high calorific value and clean combustion products, is expected to play a crucial role in future energy structure.[7–10] Currently, mainstream hydrogen production processes fall into three main categories: hydrocarbon reforming and pyrolysis, biomass processes, and hydrolysis. Although hydrocarbon reforming and pyrolysis are the most mature hydrogen production processes, they generate carbon by-products and are highly dependent on fossil fuels.[11] Water electrolysis is a promising future technology due to its environmental friendliness, lack of carbon emissions, and ease of industrial implementation (Fig. 1a).[18] At this stage, the principle research and technical route of direct water electrolysis have become increasingly mature.[19] However, since freshwater resources on the planet only account for 3.5% of the total water, using seawater for hydrogen production can lessen the tension of freshwater resources.[20] At the same time, renewable seawater resources can support the electrolysis of seawater for hydrogen production to embark on the path of sustainable development. In addition, due to the poor electrical conductivity of freshwater, conventional water electrolysis technology requires the addition of acid, base, or buffer solution to freshwater before electrolysis operation.[21] In contrast, seawater is rich in chloride ions (Cl^-), sodium ions (Na^+), magnesium ions (Mg^{2+}), sulfate ions (SO_4^{2-}), and calcium ions (Ca^{2+}). The presence of these ions significantly increases the conductivity of seawater, making it a suitable electrolyte for the electrolysis reaction. Therefore, direct electrolysis of seawater for hydrogen production has essential research value[22] (Scheme 1).

However, seawater electrolysis also faces some challenges, as described below. Firstly, seawater electrolysis mainly involves two half-reactions: HER at the cathode and OER at the anode.

[a]School of Chemical Engineering, Ocean and Life Sciences, Dalian University of Technology, Panjin 124221, China. E-mail: liuanmin@dlut.edu.cn; renxuefeng@dlut.edu.cn

[b]Shandong Engineering Research Center of Green and High-value Marine Fine Chemical, Weifang University of Science and Technology, Weifang 262700, China. E-mail: cjli@wfust.edu.cn

[c]Department of Chemistry, Tsinghua University, Beijing, 100084, China

[d]MIIT Key Laboratory of Critical Materials Technology for New Energy Conversion and Storage, State Key Laboratory of Urban Water Resource and Environment, School of Chemistry and Chemical Engineering, Harbin Institute of Technology, Harbin 150001, China. E-mail: yangpeixia@hit.edu.cn

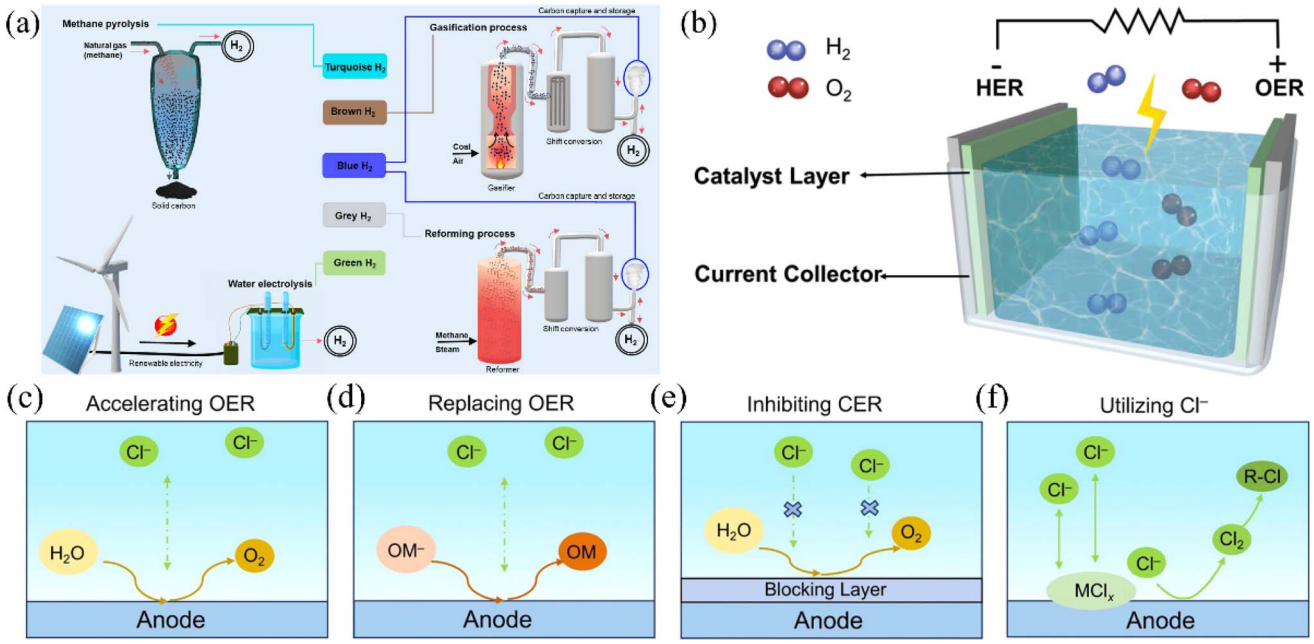

Fig. 1 (a) Various processes for making hydrogen, where electrolysis of water to make hydrogen produces green hydrogen gas. Reproduced with permission.[12] Copyright 2021, Springer Nature. (b) Diagram of a water electrolysis unit in which the hydrogen precipitation reaction occurs at the cathode and the oxygen precipitation reaction occurs at the anode. Reproduced with permission.[13] Copyright 2021, Wiley-VCH. (c) Corrosion-resistant strategies on the anode. Preparation of high-activity catalysts to increase the selectivity of the OER. (d) Finding other oxides to undergo thermodynamically more favorable oxidation reactions on the anode instead of the OER. (e) Construct a protective layer resistant to chloride ion corrosion to stop the CER. (f) The use of free chloride ions to reconstitute the catalyst or the use of *in situ*-grown chloride ions to participate in the reaction. Reproduced with permission.[14] Copyright 2023, American Chemical Society.

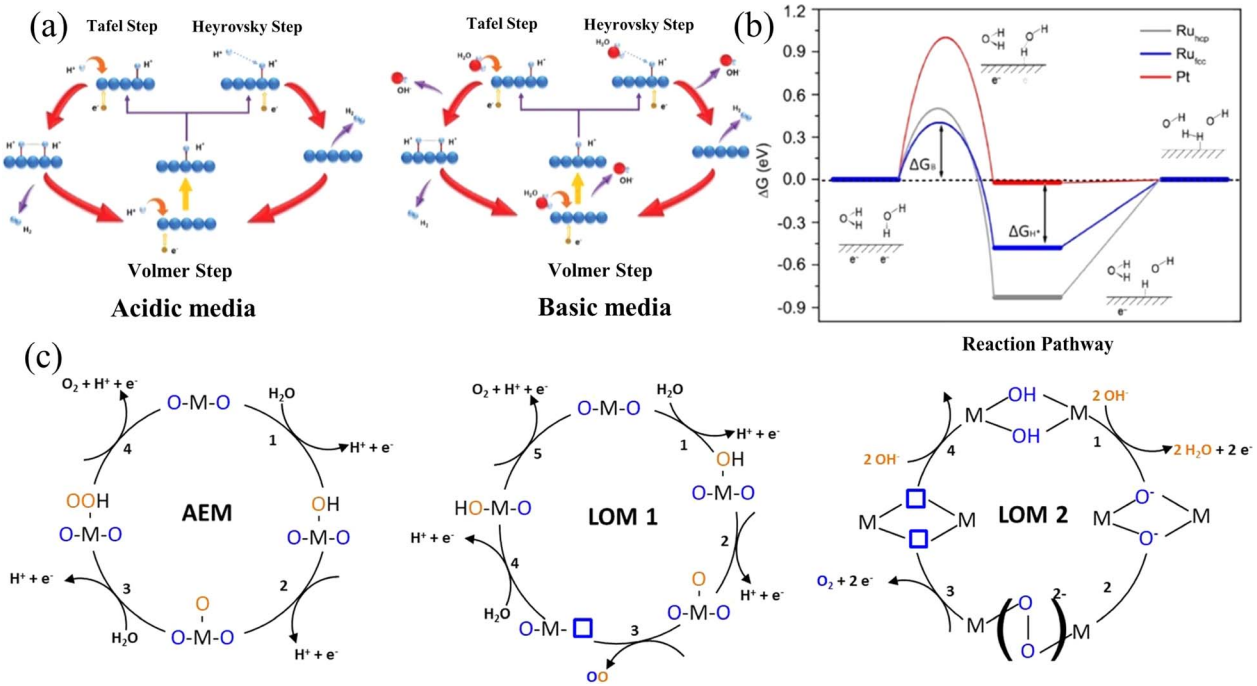

Fig. 2 (a) Reaction pathways of HER in acidic and basic media. Reproduced with permission.[15] Copyright 2021, Wiley-VCH. (b) Illustration of ΔG_{H^*} on various surfaces, depicting the reactant beginning state, intermediate state, final state, and an additional transition state symbolizing water dissociation. Reproduced with permission.[16] Copyright 2021, American Chemical Society. (c) AEM, LOM_1 and LOM_2 mechanisms of the OER. Reproduced with permission.[17] Copyright 2023, Springer Nature.

Scheme 1 Research advance of Ni-based catalysts for HER in seawater.

Nevertheless, both half-reactions are thermodynamically upslope while not being kinetically favorable. Therefore, efficient catalysts are usually needed to lower the thermodynamic energy barrier and increase the reaction rate (Fig. 3a and b).[23,27–30] These highly efficient catalysts work by lowering the thermodynamic energy barrier of the reaction, thereby reducing the energy input required for the reaction and increasing the reaction rate. The catalytic activity and stability of the catalysts can be improved by modifying the structure and composition of the catalysts and further modifying the electronic structure of the catalysts. A recent study demonstrated that introducing a Lewis acid layer (*e.g.*, Cr_2O_3) on transition metal oxide catalysts can enhance the local reaction environment, promoting stability and performance in direct seawater electrolysis.[31] Additionally, adjusting the interfacial structure of metal oxide substrates has been identified as a crucial strategy for inducing electronic structure reconstruction in supported catalysts, significantly enhancing their catalytic activity.[32] Secondly, two primary challenges are encountered in HER. On the one hand, to speed up the kinetic reaction, it is necessary to enhance the electrical conductivity of the catalyst to promote the charge transfer mechanism and consequently boost the reaction rate. The catalyst's conductivity can be enhanced by strategically structuring its structure and composition, enhancing electron conduction pathways, or using conductive additives. On the other hand, microorganisms and ions in seawater can cause the formation of insoluble compounds on the catalyst's surface, which can block active sites and decrease the catalyst's activity. To ensure durability, it is essential to use electrode materials that strongly resist corrosion from seawater and pollutants and implement corrosion resistance techniques on them.[33] Common corrosion resistance strategies on anodes are illustrated in Fig. 1c. Thirdly, for the OER at the anode, seawater is rich in halogen ions. Taking the most abundant chloride ion

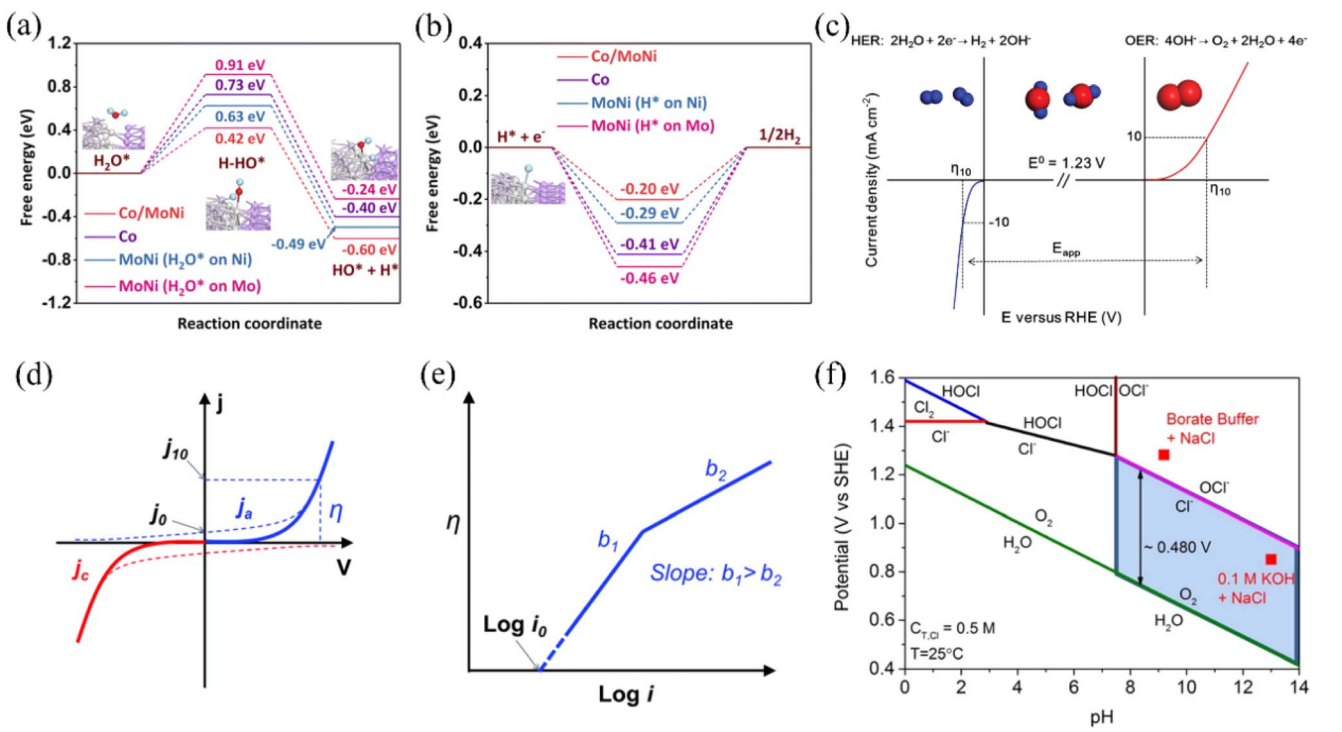

Fig. 3 (a) Water dissociation energy barrier diagrams for Co, MoNi and Co/MoNi. (b) Hydrogen adsorption energy barriers for Co, MoNi and Co/MoNi. Reproduced with permission.[23] Copyright 2023, Royal Society of Chemistry. (c) Typical HER and OER polarisation curves are shown as well as overpotentials at a current density of 10 mA cm^{-2} Reproduced with permission.[24] Copyright 2017, Wiley-VCH. (d) Polarisation curves for cathode (left) and anode (right) electrodes, j_0 is the exchange current at $j_a = -j_c$. (e) Tafel slope. Reproduced with permission.[25] Copyright 2017, Royal Society of Chemistry. (f) Pourbaix diagram of the artificial seawater model at 0.5 M NaCl. Reproduced with permission.[26] Copyright 2016, Wiley-VCH.

among them as an example, when the pH of the electrolyte is in the acidic range, Cl^- will be oxidized to chlorine gas at the anode ($2Cl^- \rightarrow Cl_2 + 2e^-$); when the pH of the electrolyte is in the alkaline range, Cl^- will be transformed to ClO^- ($Cl^- + 2OH^- \rightarrow ClO^- + H_2O + 2e^-$). The presence of chloride ions reduces the selectivity of the OER.[34,35] Although OER is superior to Chlorine Evolution Reaction (CER) in terms of thermodynamic mechanism, CER has kinetic advantages as it involves only two electrons, making it more favorable than the four-electron transfer process in OER.[36] Although the kinetically faster CER accelerates the electron reaction and promotes hydrogen production at the cathode, the generated Cl_2 and ClO^- corrode the electrodes. This corrosion leads to reduced catalyst activity or even deactivation, which is inherently unfavorable for the continuation of the reaction.[37]

An urgent requirement exists to synthesis catalysts with high catalytic activity and strong corrosion resistance for seawater electrolysis, considering the constraints mentioned above. Currently, platinum (Pt) is found to be the most efficient catalyst for HER, while IrO_x and RuO_x are considered to be the most efficient catalysts for OER.[38–40] However, these catalysts are precious metal catalysts, which are not conducive to large-scale industrialization. In recent years, researchers have found that transition metal electrocatalysts, which have good performance in the electrolysis of seawater and are abundantly available, make ideal raw materials for electrocatalysts. Among these, nickel-based materials, located in the first row of transition metals, are the most widely researched of all non-precious metal transition metal-based catalysts due to their excellent electrical conductivity and corrosion resistance.[41] Nickel oxide, nickel hydroxide, nickel phosphide, and nickel sulfide are affordable compounds that show potential as effective catalysts for seawater electrolysis.[42] Researchers have modified nickel-based materials to increase their electrochemical activity through doping modification, vacancy engineering, surface modification, and other strategies.[43,44] According to recent reports, researchers have found that intercalation in 2D materials has shown promise in enhancing the properties of electrocatalysts, providing a pathway to tailor the electronic structure and improve catalytic performance.[45] Numerous explorations have aimed at replacing precious metal catalysts with nickel-based materials, making it possible to use them as HER catalysts, OER catalysts, and even bifunctional catalysts.[46] For example, Chen *et al.*[47] found that covering a S-doped $Fe(OH)_3$ layer on NiSe nanowires can provide many active sites for nickel-based materials and improve their corrosion resistance. Liu *et al.*[48] constructed heterostructure CoP/Ni_2P@NF on Ni_2P materials, and they found that the coupling of CoP and Ni_2P optimized the electronic structure of the catalyst's active site and endowed it with excellent HER catalytic performance. Gopalakrishnan *et al.*[49] synthesized Co–Ni–S/NF *in situ* on nickel foam through a self-templating strategy. The catalyst showed outstanding efficiency in catalyzing both HER and OER due to the combined impact of the bimetal and the effective interfacial layer between the nanomaterials. However, research on nickel-based materials is still in the laboratory stage and needs to be further explored to meet the high volume of industrial production. In addition, enhancing the corrosion resistance and stability of catalysts in seawater environments is also a research priority to promote the early commercialization of nickel-based materials.

Previous reviews in this field have primarily focused on the general mechanisms of seawater electrolysis and the performance of various catalyst materials without delving deeply into nickel-based materials.[50,51] For example, unlike a recent review that focused on the impact of seawater composition on electrolysis technologies, this review provides a detailed analysis of material-specific strategies for improving catalyst performance.[52] Specifically, it targets the unique properties and enhancements of nickel-based catalysts, making it distinct and highly relevant for researchers focused on non-precious metal electrocatalysts. Additionally, this review comprehensively outlines current progress in improving the catalytic efficiency of nickel-based materials for seawater electrolysis using modification approaches. It also discusses the corrosion resistance methods used for nickel-based materials in seawater conditions. By elucidating the application of diverse strategies and principles, it serves as a valuable resource offering insights and guidance for designing and enhancing more effective nickel-based electrocatalytic materials, thereby fostering the progress of seawater electrolysis technology. Furthermore, the consolidation of corrosion resistance information can contribute to improving the stability and long-term reliability of nickel-based materials within the seawater electrolysis setting.

2. Principle of electrolysis of seawater

To understand seawater electrolysis, it is first necessary to understand the chemical reactions involved and the associated mechanisms. In addition, catalyst performance parameters, such as electrochemical surface area (ECSA), will directly affect the efficiency of seawater electrolysis and the hydrogen production rate. Therefore, understanding the evaluation of catalyst performance parameters is essential to optimize the efficiency of the seawater electrolysis process. In the following, we will elaborate on the principles of seawater electrolysis, the chemical reactions involved, and the importance of catalyst performance parameters.

2.1 Reaction equation and mechanism of electrolysis of seawater

The main principle of seawater electrolysis is based on the electrolysis of water. Electrolysis of water is usually performed in an electrolyzer, which consists of two electrodes (cathode and anode) and an electrolyte solution (Fig. 1b).[53] The theoretical potential required to electrolyze water is 1.23 V under standard conditions. However, the potential needed for the actual process will be higher than the theoretical potential, and this extra voltage beyond the theoretical potential is known as the overpotential.[54] In the electrolysis process, by applying voltage to the electrolyte to make it undergo electrolytic reaction on the electrode material, H^+ in the solution migrates to the cathode and is reduced to H_2, and OH^- migrates to the anode and is

oxidized to O_2. The reaction equation is as follows, where the voltage values provided in eqn (2) to (5) are relative to the standard hydrogen electrode (SHE):

Total reaction equation:

$$2H_2O(l) \rightarrow 2H_2(g) + O_2(g) \quad (1)$$

OER in alkaline environments:

$$4OH^- \rightarrow 2H_2O + O_2 + 4e^- \quad E^0_{anode} = 0.4\ V \quad (2)$$

OER in acidic environments:

$$2H_2O \rightarrow 4H^+ + O_2 + 4e^- \quad E^0_{anode} = 1.23\ V \quad (3)$$

HER in an alkaline environment:

$$2H_2O + 2e^- \rightarrow 2OH^- + H_2 \quad E^0_{cathode} = -0.83\ V \quad (4)$$

HER in an acidic environment:

$$2H^+ + 2e^- \rightarrow H_2 \quad E^0_{cathode} = 0\ V \quad (5)$$

The Nernst equation $\left(E = E^0 - \frac{RT}{nF}\ln Q\right)$ shows that the different electrode potentials (E) under acidic and basic conditions are mainly due to the different concentrations of H^+ and OH^-.[55] These concentration changes will affect the reaction quotient Q, thereby altering the electrode potential. The HER at the cathode is a two-electron transfer process regardless of the pH conditions. Under an acidic medium, the Volmer reaction occurs first, protons are first adsorbed on the active sites on the catalyst surface to form active H*. This is followed by the Tafel/Heyrovsky reaction to generate hydrogen, where two molecules of active H* are required to generate one molecule of H_2 in the Tafel process, while one molecule of H^+ is required to combine with one molecule of H* to generate one molecule of H_2 in the Heyrovsky process.[56] In an alkaline environment, the Volmer reaction also occurs first, with the difference that at this point, water molecules, rather than protons, adsorb on the active sites on the catalyst surface to give active H*. This is followed by the Tafel/Heyrovsky reaction to generate hydrogen, where two molecules of active H* are required to generate one molecule of H_2 in the Tafel process. In contrast, one molecule of H_2O is required to combine with one molecule of H* to generate one molecule of H_2 in the Heyrovsky process.[57] Fig. 2a illustrates the process, and the reaction equation is shown below:

In acidic environments:

Volmer reaction:

$$H^+ + e^- + * \rightarrow H^* \quad (6)$$

Tafel reaction:

$$2H^* \rightarrow 2^* + H_2 \quad (7)$$

Heyrovsky reaction:

$$H^* + H^+ + e^- \rightarrow * + H_2 \quad (8)$$

In alkaline environments:

Volmer reaction:

$$* + H_2O + e^- \rightarrow H^* + OH^- \quad (9)$$

Tafel reaction:

$$2H^* \rightarrow 2^* + H_2 \quad (10)$$

Heyrovsky reaction:

$$H^* + H_2O + e^- \rightarrow * + OH^- + H_2 \quad (11)$$

The Gibbs free adsorption energy of H* (ΔG_{H^*}) is commonly used in HER to react with the electrochemical properties of catalysts.[58] The larger the negative deviation of the value of ΔG_{H^*} from zero, the stronger the adsorption behavior of H*, while the larger the positive deviation, the weaker the adsorption behavior of H*. When the value of ΔG_{H^*} is too small, it favors the Volmer reaction but is unfavorable for the subsequent Tafel/Heyrovsky reaction. Conversely, if the value is too large, the Volmer reaction cannot easily occur, reducing the amount of H* available for the subsequent reaction, which is macroscopically unfavorable to the HER. When ΔG_{H^*} is closer to 0 indicates that the HER performance of the catalyst is better (Fig. 2b). The researchers found that acidic conditions are more favorable for HER, however, nickel-based materials are more susceptible to corrosion under acidic conditions than alkaline conditions.[59,60] So, the focus in the study of HER catalysts for nickel-based materials is to enhance their corrosion resistance or to prepare catalysts under alkaline conditions to meet industrial needs, which can be done by metal doping to modulate the electronic structure of the active site to bring ΔG_{H^*} closer to 0. In addition, in seawater, which is rich in a large number of microorganisms and other ions, the pH near the cathode fluctuates during seawater electrolysis, which can cause cations such as Mg^{2+} and Ca^{2+} in seawater to generate insoluble $Mg(OH)_2$ and $Ca(OH)_2$ to cover the electrode surface, blocking the active sites on its surface. To address the aforementioned challenges, it is imperative to optimize the electrolysis conditions or implement alternative measures to avert poisoning and deactivation of the catalyst.

Compared to the two-electron transfer HER process, the OER process (Fig. 2c) involving four-electron transfer has a slower reaction rate. The figure illustrates three distinct OER mechanisms: the Acidic Environment Mechanism (AEM), Lattice Oxygen Mechanism 1 (LOM 1), and Lattice Oxygen Mechanism 2 (LOM 2). In the AEM, hydroxyl groups (OH^-) form on the metal-oxide surface, which subsequently release oxygen (O_2), hydrogen ions (H^+), and electrons (e^-).[61] The LOM 1 involves lattice oxygen atoms forming a peroxo species (O–O) that bridges metal-oxide sites and then decomposes to release oxygen (O_2). Meanwhile, in LOM 2, two hydroxyl groups (OH^-) combine to form a peroxo species (O–O), which also decomposes to release oxygen (O_2).[62] These mechanisms underscore the complexity and multistep nature of the OER, significantly contributing to its slower reaction rate compared to the HER. This highlights the critical need for developing more efficient

and stable catalysts for water splitting applications. In addition, seawater is more than 55% chloride, and there are also other anions such as sulfate ions, bromide, *etc.* These anions compete with the OER at the anode.[63] Below, we describe the CER during the electrolysis of seawater using the reaction equation for chloride ions as an example. The reaction equation is as follows:

In strongly acidic environments (pH < 3)

$$2Cl^- \rightarrow Cl_2 + 2e^- \quad E^0_{anode} = 1.36\ V \tag{12}$$

In a weakly acidic environment (3 < pH < 7.5)

$$Cl^- + H_2O \rightarrow HClO + H^+ + 2e^-$$
$$E^0_{anode} = (1.494 - 0.0295\ pH)\ V \tag{13}$$

In alkaline environments (pH > 7.5)

$$Cl^- + 2OH^- \rightarrow ClO^- + H_2O + 2e^-$$
$$E^0_{anode} = (1.795 - 0.0591\ pH)\ V \tag{14}$$

Although the kinetically more favorable CER can macroscopically accelerate the reaction rate and promote hydrogen production, chloride ions are corrosive and can cause severe damage to the electrodes. Based on the Pourbaix diagram (Fig. 3f), Dionigi *et al.* found that the potential difference between hypochlorite and oxygen under alkaline conditions, when pH > 7.5, is fixed at 0.48 V, and they proposed that the difference between the OER and the standard potential for hypochlorite generation (ΔE^0) be used as the condition for the selective operation of the OER.[26] In other words, the reaction under alkaline conditions is more favorable for improving the selectivity of the OER and inhibiting the reaction of CER. Developing electrocatalysts with high selectivity and corrosion resistance is crucial due to seawater's corrosive nature of free chlorine ions, which can degrade electrode materials.[64] This advancement is essential for reducing corrosion effects and improving electrolysis procedures' effectiveness.

2.2 Evaluation of catalyst performance parameters

In evaluating the catalytic performance of OER/HER electrocatalysts, the catalytic performance can be evaluated by the following important parameters: initial potential and overpotential, current density, Tafel slope, Faraday efficiency (FE), electrochemical surface area, and catalyst stability.

2.2.1 Initial potential and overpotential. The initial potential (E) is the turning point on the polarization curve (or cyclic voltammetry) from a non-Faraday current to a Faraday current. Overpotential (η) is the fraction of the actual potential greater than the theoretical potential required to achieve a certain current density in an electrochemical reaction (Fig. 3c). For HER and OER, the overpotential is the portion of the potential greater than the standard electrode potential required at a current density of 10 mA cm^{-2} in order for the corresponding water reduction or oxygen precipitation reaction to take place at the electrode, and its unit is usually expressed in the voltage unit V. In general, a low onset/overpotential means that the catalyst can start promoting reactions at a low potential, which reflects the high activity and efficiency of the catalyst. Conversely, it means that the catalyst is less active. In electrochemical experiments, the starting potential and overpotential of a catalyst can be read from its LSV curve. The overpotential of a catalyst is influenced not only by its intrinsic activity but also by elements like the electrolyte environment. Therefore, relying solely on this parameter to assess the catalyst's performance may be inadequate.

2.2.2 Current density. Current density (J) is the value of current passing through a unit area, usually in mA cm^{-2}. Current density can directly reflect the activity and efficiency of a catalyst in catalyzing a reaction. A high current density means that the catalyst is able to promote the reaction at a higher rate, while a low current density may mean that the catalyst is inefficient or less active. However, high current densities are often accompanied by more severe electrochemical corrosion and the generation of large numbers of bubbles, which can damage the catalyst. Therefore, researchers need to select suitable catalyst carriers or add adhesives to enhance adhesion properties and use corrosion-resistant materials to enable electrocatalysts to reach higher current densities. Similarly, the LSV curve can reflect the current density of the catalyst at different potentials.

2.2.3 Tafel slope. According to the Tafel equation ($\eta = a + b\ lg(|j|)$), where a is the Tafel constant, the Tafel slope (b) reflects the potential difference required for each tenfold increase in current density (Fig. 3e). In electrochemical experiments Tafel slope can be obtained by fitting LSV curves, the smaller the value the smaller the overpotential required for the surface to reach the same current density and the faster the reaction rate. In addition, according to the Butler–Volmer equation, it is known that the magnitude of the Tafel slope can be used to determine the decisive speed step in the reaction process and reveal the corresponding mechanism of the reaction. High-performance electrocatalysts often demonstrate characteristics such as higher current density and lower Tafel slope, as shown in Fig. 3d.

2.2.4 Faraday efficiency. FE is the efficiency with which energy is transferred from electrical energy to chemical energy and stored in the product oxygen/hydrogen gas. That is, the ratio between the experimentally produced oxygen/hydrogen gas and the theoretically calculated gas volume is a measure of the efficiency of the applied current to drive the expected OER/HER. The actual gas production can be determined by the water–gas displacement method and the gas chromatography (GC) method, and the theoretical gas production can be calculated by Faraday's second law.[65,66] Due to the presence of chloride ions in the seawater, a CER occurs at the anode, which can reduce the Faraday efficiency. Faraday efficiency is an important indicator of catalyst activity and efficiency. A high Faraday efficiency is crucial for catalysts as it indicates their ability to drive the HER and OER with high efficiency. This is particularly important for enhancing the efficiency of seawater electrolysis. Achieving a Faraday efficiency close to 100% is ideal for the development of efficient catalysts. At the same time, the Faraday efficiency can also provide important information about the active sites on the catalyst surface and the reaction mechanism.

2.2.5 Electrochemical surface area. A catalyst's ECSA refers to the surface area that contains effective reactive active sites crucial for electrochemical reactions. Active sites are particular areas on the catalyst surface that can adsorb reactive chemicals and promote the intended reactions. The ECSA is critical for evaluating the catalyst's performance as it directly affects its activity and stability. A larger ECSA implies that more active sites on the catalyst are available for the reaction, leading to an increased reaction rate. The ECSA can be determined from non-Faraday currents, with one method involving the measurement of double electric layer capacitance (C_{dl}). The bilayer capacitance represents the capacitance between the electrode surface and the electrolyte. When scanning in the bilayer region, the current obtained is proportional to the scanning speed, and the slope can indicate the magnitude of the C_{dl}. The ratio of the bilayer capacitance to the capacitance of a planar electrode is defined as the roughness factor. The electrochemically active surface area can be calculated by multiplying the roughness factor with the geometric area. Generally, a larger electrochemical surface area corresponds to higher catalyst activity, highlighting the importance of ECSA in enhancing the performance of catalysts in electrochemical reactions.

2.2.6 Stability. Stability refers to the ability of a catalyst to maintain its performance and structure over long periods of operation or cycling. Catalyst stability is critical in evaluating catalyst performance because prolonged use can lead to gradual deterioration of catalyst performance or structural damage, reducing the efficiency of the electrolysis process. Because seawater contains a variety of salts and impurities, these components may cause corrosion, scaling, or other undesirable reactions to the catalyst, affecting its performance and lifetime. Therefore, the stability of catalysts in electrolyzed seawater needs to be carefully evaluated. The stability of electrocatalysts is usually characterized using several methods, including chrono-potentiostatic (CP) and chronoamperometry (CA). In CP, the stability of catalysts in electrolytic seawater can be assessed by applying a stabilized potential during the electrolysis reaction to simulate the catalyst's prolonged operation. By monitoring the change in current over time, the change in performance of the catalyst during long time operation can be assessed, as well as its stability. In CA, a constant current is applied, and the change in potential is monitored over time. This method helps in understanding the durability of the catalyst under constant operational conditions and provides insights into how the catalyst's performance changes due to potential corrosion or other degradation processes in seawater. In addition, accelerated cyclic voltammetry (CV) and long-term galvanostatic electrolysis are also effective methods to assess electrocatalyst stability. CV involves applying different voltage ranges through multiple cycles in a short period to simulate long-term usage, with changes in CV curves indicating stability and performance in seawater. Long-term galvanostatic electrolysis applies a constant current over an extended period, monitoring resulting voltage changes to evaluate durability under continuous seawater operation.

The catalytic performance of OER/HER electrocatalysts can be evaluated based on the critical parameters mentioned above. The initial potential and overpotential indicate the catalyst's activity level, while current density reflects its efficiency in promoting reactions. The Tafel slope reveals the potential difference required for increased current density and helps determine the reaction mechanism. Faraday efficiency measures the energy transfer efficiency in driving OER/HER. The electrochemical surface area indicates the active sites available for reactions, and catalyst stability is crucial for maintaining performance over time, especially in seawater electrolysis. Stability assessments involve monitoring performance changes during prolonged operation and resistance to corrosion and degradation.

3. Nickel-based electrocatalysts

The intricate four-electron transfer process of OER, coupled with the challenge of excessive overpotential and the competition with CER on the anode, have emerged as significant research bottlenecks impeding the commercial advancement of hydrogen production from electrolytic seawater.[61] Additionally, it is necessary to research HER catalysts that have a greater number of active sites. Developing electrocatalysts with high catalytic activity and stability can reduce the energy barrier of the reaction and speed up the process, which is an important area of research.[15,17] More rational strategies have been designed from different perspectives to address the above challenges to meet the large-scale commercialization needs of electrolytic seawater. Nickel-based materials show great potential as electrocatalysts due to their plentiful availability, cost efficiency, environmental friendliness, and the ability to control their electrical structure easily. For example, Liang *et al.* synthesized highly efficient HER catalysts from nickel-doped tungsten oxide nanorods (Ni–WO_x) using the property that Ni doping can optimise the activity of hydrogen precipitation reactions (Fig. 4d–g).[69] In electrocatalysis, many electrocatalysts based on nickel-based materials have demonstrated striking bifunctional properties compared with traditional electrocatalysts. Specifically, many nickel-based catalysts are not only able to catalyze OER effectively but also able to catalyze HER simultaneously in the same system. Therefore, nickel-based catalysts have attracted much attention in electrocatalysis research and offer new possibilities for achieving efficient energy conversion (Fig. 4a–c).[67,70]

In practical applications, nickel-based materials still face some challenges as electrocatalysts, such as the low electronic conductivity of a single nickel-based material and the insufficient stability of synthesized electrode materials.[71] Therefore, the current research focuses on modifying nickel-based materials by regulating the morphology of nickel-based materials, doping with metallic elements or non-metallic elements to construct efficient nickel-based catalysts, and controlling the reaction kinetics.[72] This section provides an overview of the design and synthesis, structural characterization, and methods to improve the catalytic efficiency of metal-doped, non-metal-doped, and other nickel-based catalysts for OER and HER.

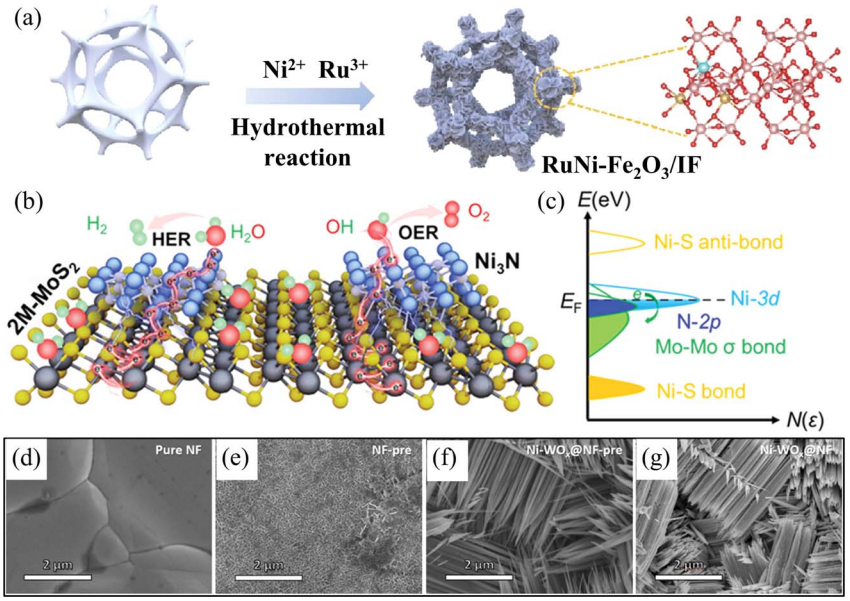

Fig. 4 (a) Synthesis of bifunctional RuNi–Fe_2O_3/IF by hydrothermal method. Reproduced with permission.[67] Copyright 2022, Elsevier. (b) Schematic illustration of water splitting process of the Ni_3N@2M-MoS_2. (c) A proposal for charge modulation of active electronic states in Ni_3N@2M-MoS_2 with bifunctionality. Reproduced with permission.[68] Copyright 2022, Wiley-VCH. (d) SEM image of NF. (e) SEM image of NF-pre. (f) SEM image of $NiWO_x$@NF-pre. (g) SEM image of Ni–WO_x@NF. Reproduced with permission.[69] Copyright 2023, Elsevier.

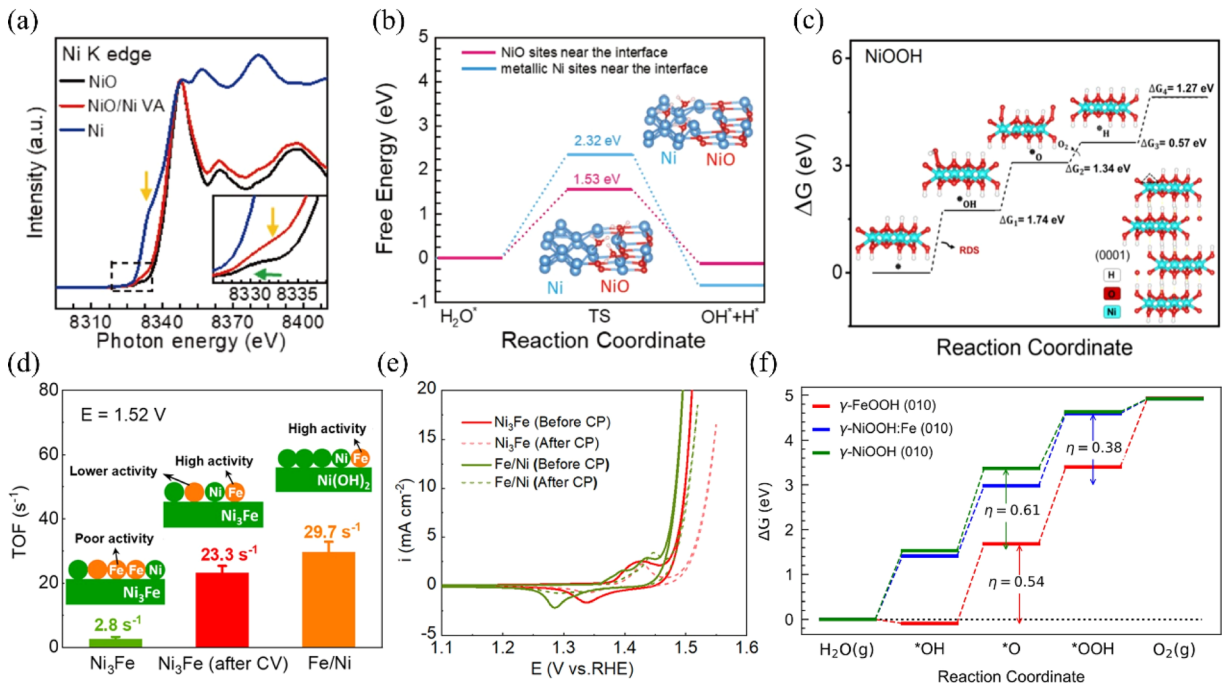

Fig. 5 (a) The nickel K-edge X-ray absorption spectroscopy (XAS) technique can be used to characterize NiO, Ni/NiO VAN, and Ni hybrid systems. (b) Calculations have revealed the energy barriers for water dissociation kinetics at metallic Ni sites and NiO sites located near the interface. Reproduced with permission.[74] Copyright 2022, Springer Nature. (c) The OER free-energy diagrams at $U = 1.23$ V for the O-terminated NiOOH surface have been calculated, using the LOM mechanism. Reproduced with permission.[75] Copyright 2023, American Chemical Society. (d) TOF values for uncirculated Ni_3Fe, Ni_3Fe after 10 cycles between −0.4 and 1.45 V, and Fe/Ni(O) hydroxide catalysts. (e) The OER CV curves of Fe/Ni and Ni–Fe (oxy)hydroxides before and after the CP test. Reproduced with permission.[76] Copyright 2022, American Chemical Society. (f) The theoretical OER free energy diagram for NiOOH, FeOOH, and Fe-doped NiOOH has been constructed. Reproduced with permission.[77] Copyright 2023, American Chemical Society.

3.1 Nickel-based catalysts for OER

For the OER, nickel-based materials are potential OER catalysts for electrolytic seawater due to their tunable three-dimensional (3D) electronic configurations, diverse crystal structures, and highly reactive end states during the OER process.[73] Researchers have constructed efficient nickel-based catalysts and modulated reaction kinetics by tuning the morphology of nickel-based materials, doping metallic elements, or modifying nickel-based materials with non-metallic elements. This section summarizes the domestic and international reports of OER catalysts in recent years.

3.1.1 Nickel-based oxides and layered double hydroxides. Recently, significant research have been achieved on nickel-based oxides (NiO) in OER, and various strategies have been used to improve their catalytic OER activity. NiO exhibit efficient catalytic activity for the OER by leveraging the synergistic effect at the interface between nickel and nickel oxide (Fig. 5a). This effect lowers the energy barrier for hydrolysis dissociation and promotes the creation of intermediate products (Fig. 5b).[74,78] Based on the morphology theory, Khadijeh *et al.*[75] developed nanorod array-based hierarchical NiO microspheres to turn bare nickel foam into hydrophilic NiO. This procedure can transform the nickel foam surface into a complex porous structure like a sea urchin, enhancing surface area, active sites, and corrosion resistance (Fig. 5c). The catalyst exhibited high stability and selectivity throughout a continuous week of electrolysis. Furthermore, the study illustrated the effectiveness of Ni–Fe oxides as anode materials. Theoretical analysis indicated that the incorporation of Fe at the edge of Ni oxides not only enhances the turnover frequency (TOF) but also improves the durability compared to single-metal Ni oxides (Fig. 5d and e).[76] Zhang *et al.* prepared a nickel oxide catalyst, Fe–NiO_xH_y/CC, doped with a small amount of Fe. The overpotential required for this catalyst was only 206 mV under simulated seawater conditions at a current density of 10 mA cm^{-2}.[77] In addition, the catalyst showed remarkable stability in simulated seawater. The researchers analyzed the catalyst by density functional theory (DFT) calculations. They learned that the presence of Ni–Fe bridging sites in the catalyst can regulate the precipitation of Cl*, which is beneficial to increase the OER activity (Fig. 5f). In addition, the construction of defective structures can provide additional reaction centers to electrify the coordination environment of atoms on the catalyst surface, which in turn modulates the electronic structure. The NiO_x–FeO_x nanocomposites synthesized by Haq *et al.* require only 380 mV overpotential to achieve a current density of 1000 mA cm^{-2}, which is better than the overpotential required for IrO_2 at this current density.[79] Additionally, the catalyst is protected by g-C_3N_4, which helps resist pitting and stress corrosion at the anode, providing high corrosion resistance. The 3D hierarchical porous structure of g-C_3N_4 provides a short diffusion channel for ion transfer and mass transport, which is very favorable for seawater penetration. At the same time, the amorphous NCs have a unique self-healing and flexible structure to further improve corrosion resistance.

Based on the study of electrolyzed water, the researchers found that under alkaline circumstances, nickel–iron layered double hydroxide (NiFe-LDH) exhibits strong catalytic activity and stability for the OER.[80–82] LDHs (layered bimetallic hydroxides) are interlayer structures consisting of positively charged bivalent metal ions and negatively charged oxide ions (*e.g.*, hydroxide ions) arranged in a specific ratio (Fig. 6a). This unique structure allows LDHs to have a rich and tunable active surface. Also, it provides channels for the transfer of electrons and ions, which facilitates the rapid release of hydrogen and oxygen produced in the electrolysis reaction of water.[85] However, due to the positively charged surface of LDHs, negatively charged chloride ions may be adsorbed on the surface during the electrolysis of seawater, resulting in the corrosion of the catalysts.[86,87] Yao *et al.* introduced Ce into nickel foam NiFe LDH arrays to obtain Ce–NiFe LDH/NF, a strong electrocatalyst for seawater OER. The introduction of Ce serves dual roles during seawater electrolysis: it promotes the formation of the amorphous reactive material NiOOH, while simultaneously generating CeO_2, which effectively inhibits carbonate evolution currents (CECs) (Fig. 6b and c).[83] Different strategies to improve the OER performance of NF-LDH include the doping of high valence metal ions such as Mo and V. High valence metals can induce the formation of amorphous structures in nickel-based materials, or form defects and lead to the formation of oxygen vacancies, which increase the active sites.[72] Qi *et al.* demonstrated that by intercalating hexavalent molybdenum ions Mo(VI) in NF-LDH, $MoSO_4^{2-}$ can modulate the electronic structures of Ni and Fe.[84] This lowers the OER energy barriers and promotes the generation of NiOOH, thereby increasing the active sites of OER (Fig. 6d). In summary, in recent years, researchers have used various strategies to improve their reactivity, such as interfacial synergism, morphological modulation, and elemental doping, for the application of nickel-based oxides and hydroxides on electrolytic seawater. In addition, LDHs have been shown to have excellent catalytic activity and stability under alkaline conditions. Among them, nickel-based oxide catalysts doped with elements such as aluminum, phosphorus, and iron showed good activity and stability and high electrochemical surface area. Furthermore, the doping of high-valent metals such as molybdenum and vanadium was also found to help increase the number of active sites in nickel–iron bilayer hydroxides.

3.1.2 Nickel-based phosphides. Phosphorus, sulfur, nitrogen, and other anions in nickel-based catalysts can enhance the electrical configuration and catalytic sites on the catalyst's surface, increase the conductivity, and provide suitable adsorption strength for the intermediates.[88] This section will focus on the recently reported nickel-based phosphides. Researchers have employed surface modification, nanostructure optimization, and electronic structure regulation to modify and tune nickel-based phosphides, aiming to enhance their intrinsic catalytic activity for the OER (Fig. 7h).[91–93] Liu *et al.* synthesized acicular Fe–Ni_2Pv through Fe doping and phosphorization on nickel foam, guided by DFT predictions (Fig. 7a).[89] This material demonstrated bifunctional catalysis for OER and HER in an alkaline simulated seawater electrolyte. Fe

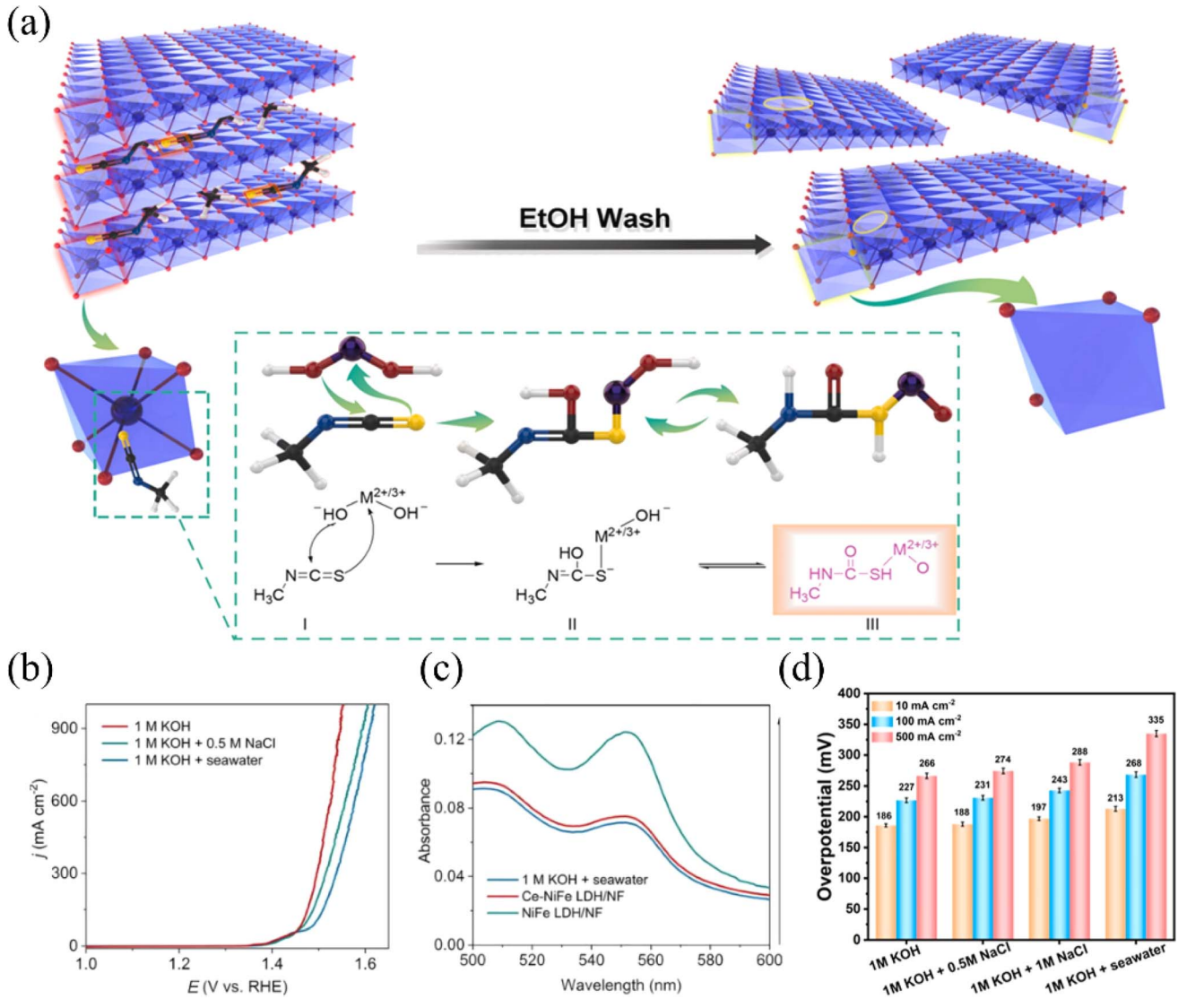

Fig. 6 (a) Designing LDHs with metal and oxygen multivacancies requires targeting specific atoms to create these vacancies. Reproduced with permission.[81] Copyright 2020, Elsevier. (b) Ce–NiFe LDH/NF was used as the catalyst, and LSV curves were measured in different electrolytes to evaluate its performance. (c) After the stability test, UV-vis absorption spectra of Ce–NiFe LDH/NF and NiFe LDH/NF electrolytes were obtained. Reproduced with permission.[83] Copyright 2024, Elsevier. (d) $Mo_{0.25}$–NiFe LDH at different current densities in different electrolytes, corresponding overpotentials were measured. Reproduced with permission.[84] Copyright 2023, American Chemical Society.

doping combined with P vacancies promotes the regeneration of active sites on the OER surface and boosts the hydrogen adsorption free energy (ΔG_{H*}) for the HER (Fig. 7b). In this case, Ni sites become the dominant OER active centers (Fig. 7c), while Fe atoms become the active centers of HER. In addition, the introduction of P vacancies also improves the electrical conductivity of this catalyst, enabling the Fe–Ni_2Pv to achieve current densities of 1.0 and 3.0 A cm^{-2} to meet the industrial requirements at a low voltage of 1.68 V and 1.73 V, respectively, in a 6.0 M KOH environment at 60 °C (Fig. 7d). Using a typical *in situ* self-assembly strategy, Yu *et al.* synthesized Ni-based heterostructured catalysts ($NiO/Ni_3S_2@Ni_5P_4$) with phosphorylated layers to enhance the OER in seawater electrolysis. They experimentally demonstrated that the overpotentials of this catalyst for the OER in freshwater and seawater at a current density of 10 mA cm^{-2} were 280 mV and 310 mV, respectively, significantly lower than those of commercial RuO_2 catalysts (Fig. 7e).[90] This catalyst has outstanding OER performance is primarily due to the electronic synergy between the NiO/Ni_3S_2 heterostructure and the phosphide layer. This synergy activates the active sites of Ni, while the outer phosphide layer enhances corrosion resistance, structural compactness, and electron transfer rate on the catalyst's surface. Therefore, the catalyst can maintain stability for 100 h at a current density of 100 mA cm^{-2} (Fig. 7f and g).

Fu *et al.* used electroplating to generate a series of Ni–P nano microspheres on an asbestos substrate that is both flexible and corrosion-resistant, and synthesized NiP_x@HA with both catalytic HER and OER functions.[94] Due to the strong chemisorption between the nickel-rich material and the two-dimensional

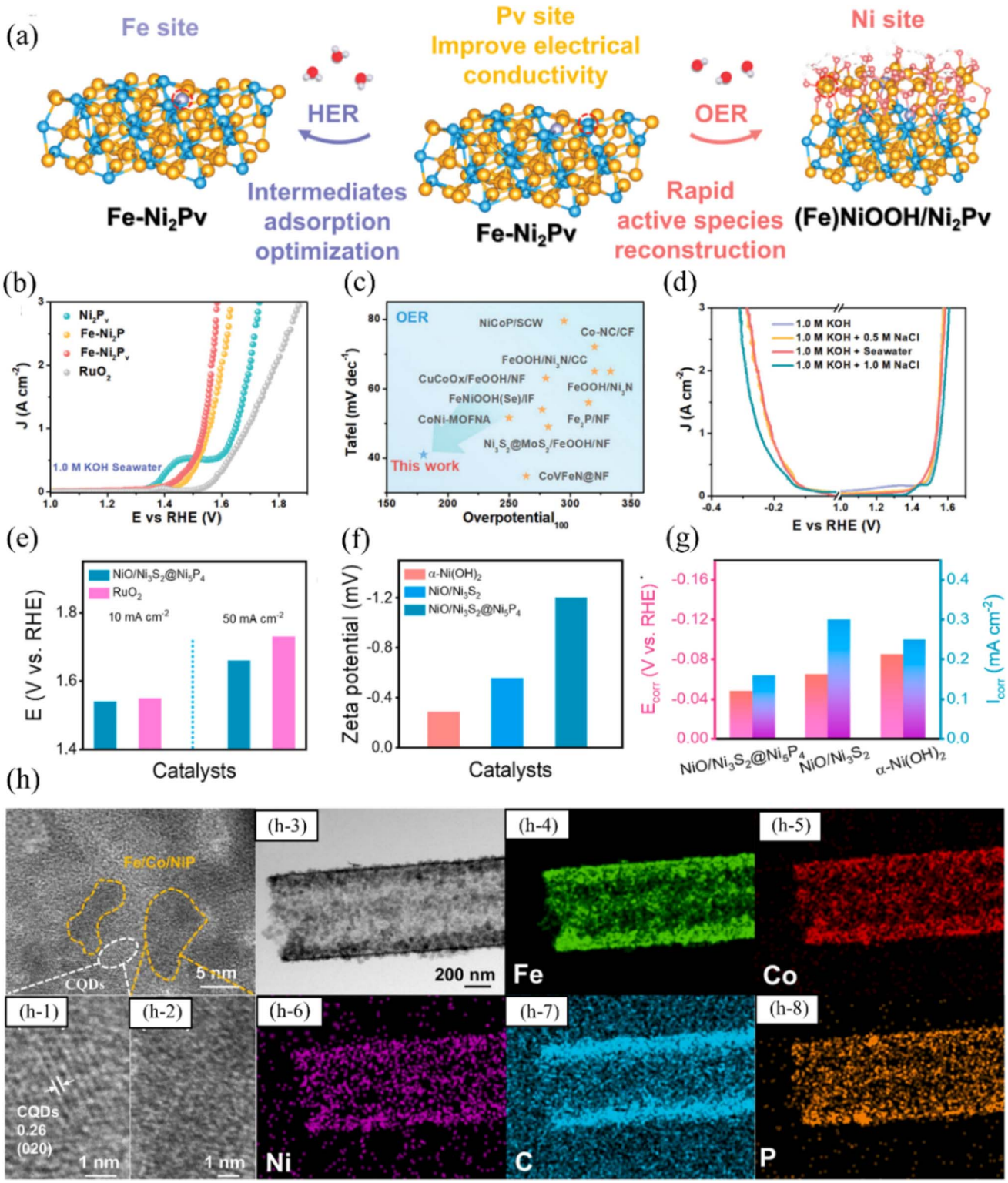

Fig. 7 (a) Fe–Ni_2Pv in 1.0 M KOH seawater electrolyte during HER and OER was represented schematically, showing the genuine phases and active sites. (b) Fe–Ni_2Pv and comparison catalysts were subjected to *iR*-compensated LSV polarization testing for OER, and the resulting curves were analyzed and compared. (c) The Tafel slope and overpotential at 100 mA cm^{-2} of the Fe–Ni_2Pv catalyst were compared with those of the recently reported OER catalysts. (d) Different electrolyte solutions were used to obtain polarization curves of the Fe–Ni_2Pv catalyst with *iR*-correction. Reproduced with permission.[89] Copyright 2023, Wiley-VCH. (e) The overpotentials for OER in seawater electrolytes were compared between NiO/Ni_3S_2@Ni_5P_4 and RuO_2 catalysts. (f) Zeta potentials of NiO/Ni_3S_2@Ni_5P_4, NiO/Ni_3S_2, and α-Ni(OH)$_2$ in seawater electrolyte. (g) The corrosion potentials and corrosion current densities in seawater electrolyte were compared among NiO/Ni_3S_2@Ni_5P_4, NiO/Ni_3S_2, and α-Ni(OH)$_2$. Reproduced with permission.[90] Copyright 2023, Elsevier. (h) Structural characterisation of FCNP@CQDs. The HRTEM images of a FCNP@CQDs: (h-1) show clear lattice spacing corresponding to the (020) plane, (h-2) show a low crystalline or amorphous phase of Fe/Co/Ni phosphide; and (h-3) TEM image of a FCNP@CQDs nanotube and the corresponding mapping for (h-4) Fe, (h-5) Co, (h-6) Ni, (h-7) C and (h-8) P. Reproduced with permission.[91] Copyright 2023, Elsevier.

layered substrate, and the hexahedral crystal structure of Ni_5P_4 enhancing electron transfer, the catalyst exhibits overpotentials of 208 mV for HER and 392 mV for OER under a current density of 200 mA cm^{-2}. Furthermore, the catalyst maintains stability for 960 h at a current density of 500 mA cm^{-2}. Moreover, large-area NiP_x-based electrodes of 22 cm × 22 cm can be synthesized using elemental doping engineering, enabling large-scale hydrogen production in alkaline seawater electrolytes. Although some progress has been made in the study of nickel-based phosphide electrocatalysts in seawater electrolysis, some challenges still need to be addressed. Firstly, consideration needs to be given to how to scale up the preparation of nickel-based phosphide electrocatalysts, which requires the development of novel and simple methods. Currently, most of the research progress has been limited to the preparation of such catalysts on a small scale, and further research on how to realize the scale-up of the structures is still needed, which is essential for practical applications. In addition, nickel-based phosphides as OER catalysts also need to improve the reaction selectivity.[95] Many studies primarily concentrate on achieving high current density in catalyst materials, often overlooking the critical issue of addressing catalyst oxidation.[96] This oversight results in the durability of the catalyst not meeting the stringent standards required for industrial applications.

3.1.3 Nickel-based sulfides. Similar to the phosphatization of nickel-based materials, many studies have been reported in recent years for sulfides of nickel-based materials. Since transition metal sulfides can be used to reconstruct the catalyst surface, based on this property, sulfide-based electrocatalysts have been successfully synthesized in direct electrolysis of water studies (Fig. 8a).[97,101] The application of bimetallic sulfides in seawater electrolysis was explored for the first time by Wang *et al.* through NiCoS NSAs prepared by a simple one-step hydrothermal method. The surface-incorporated sulfides enhanced the selectivity and corrosion resistance of the catalysts. Furthermore, the NiCoS NSAs, with their large surface area backbone structure, enabled the catalysts to achieve a current density of 800 mA cm^{-2} at a voltage of 2.08 V in natural seawater, maintaining continuous operation for 100 h (Fig. 8b and c).[98] Incorporating phosphorus and sulfur (P/S) into a single doped sulfide material exhibits a synergistic effect and robust coupling between these non-metallic elements. This unique property can be leveraged to create a nickel sulfide/phosphide interface, enabling the development of electrocatalysts for seawater electrolysis that offer both high activity and bifunctionality. Wang *et al.* prepared NiPS/NF microsphere electrocatalysts *via* a simple electrodeposition method. Phosphorization and sulfation modifications induced electron rearrangement at the heterointerface, facilitating easier adsorption of intermediates (Fig. 8d).[70] Meanwhile, NiPS/NF is a bifunctional catalyst for OER and HER, and can reach a high current density of 100 mA cm^{-2} in alkaline seawater with only 344 mV and 188 mV overpotentials, respectively, without degradation. This performance is attributed to the synergistic effect of Ni_2P and NiS_2, which imparts excellent corrosion resistance to the catalyst. Luo *et al.* synthesized Ni_3S_2/Fe–NiP_x with a spherical tesseract structure composed of nanocubes by directly etching Ni_3S_2 with potassium ferrocyanide. This unique structure exposed more active sites, and the synergistic action of P and S during the OER process created a defect-rich active intermediate layer of $Ni(OH)_2$/Ni(Fe)OOH, thereby regulating the adsorption free energies of the intermediates.[100] Ni_3S_2/Fe–NiP_x in alkaline seawater requires only 351 mV overpotential at a current density of 1000 mA cm^{-2}, with a stability of more than 225 h, and exhibits lower overpotentials (Fig. 8g). Combining the advantages of NiFe LDHs in catalyzing OER with the corrosion resistance of sulfide layers in electrolytic seawater. Sun *et al.*[99] prepared NiFe-LDH-S by altering the surface morphology of NF-LDH *via* plasma treatment technique. The transition metal sulfide layer formed on the catalyst can effectively inhibit the adsorption of chloride ions due to electrostatic repulsion. NiFe-LDH-S exhibits a minimum overpotential of 296 mV at a current density of 100 mA cm^{-2} in simulated seawater (Fig. 8e and f). It shows negligible potential drop in a 12 h continuous CP test, demonstrating corrosion resistance and stability that meet industrial requirements.

3.1.4 Nickel-based nitrides. Compared to nickel-based phosphides and nickel-based sulfides, nickel-based nitrides have slow kinetics of catalyst reactions due to the inherent chemical inertness of elemental N.[102] However, nickel-based nitrides have also demonstrated good electrochemical properties by applying vacancy engineering, metal doping, *etc.* Wang *et al.* reported a 3D multilayered heterostructured nanoarray electrocatalyst (Ni_3FeN@C/NF) (Fig. 9a) on which the N bonds contracted the d-band of the metal catalyst, obtaining a higher Fermi energy and exhibiting better electrochemical activity (Fig. 9c).[103,106] Meanwhile, the synergistic coupling between the carbon coating covered on this catalyst and the Ni_3FeN encapsulated within it ensures the electron transport flux. The final assembled electrolytic seawater tank can realize a current density of 500 mA cm^{-2} at a low cell voltage of 1.91 V (Fig. 9b). In addition to single N-doped compounds, Zhao *et al.* enhanced electrocatalytic activity by creating an interface between nitride and sulfide materials. They reported a NiNS electrode synthesized *via* a simple one-step calcination process, using nickel foam and thiourea under vacuum conditions.[104] The electrode is bifunctional with excellent catalytic properties, and the interfacial structure between Ni_3N and Ni_3S_2 served as an electrochemically active site and contributed to the dissociation and adsorption of water molecules. The overpotentials of this catalyst for HER/OER were 197 mV and 404 mV, respectively, at 100 mA cm^{-2} current, which was significantly better than those of most non-metal-based electrocatalysts, such as Ni_3N–Co and Co_3Se_4/Co (Fig. 9d). Sun *et al.* synthesized sandwich-like NiCoHPi@Ni_3N/NF by electrodepositing bimetallic nickel cobalt hydrogen phosphate (NiCoHPi) onto the surface of nickel nitride (Ni_3N) supported on nickel foam substrate.[105] The synergistic effect of the NiCoHPi deposition layer and Ni_3N substrate enhances charge redistribution and electron transfer on the catalyst surface. Additionally, vertically grown nanosheet arrays on nickel foam increase the electrocatalytic surface area, providing more active sites. At the same time, this hierarchical three-dimensional porous structure also promotes mass transfer. Therefore, NiCoHPi@Ni_3N/NF exhibits excellent

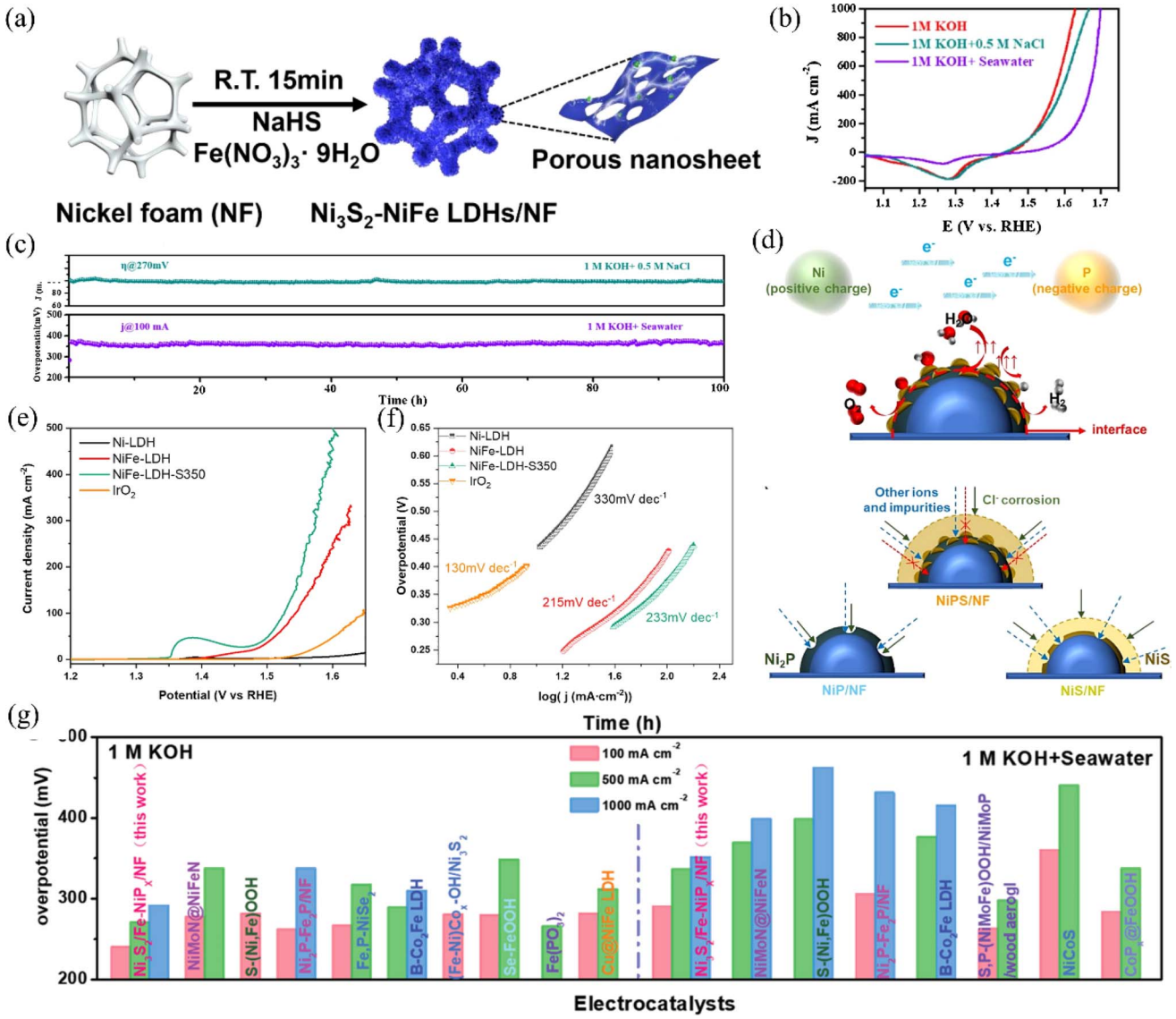

Fig. 8 (a) An illustration depicting the synthesis process of Ni_3S_2–NiFe LDHs/NF. Reproduced with permission.[97] Copyright 2022, Elsevier. (b) CV backward scan curves for the NiCoS electrode tested in different electrolytes. (c) The long-term stability of the NiCoS electrode in various electrolytes was evaluated through chronoamperometry and chronopotentiometry measurements. Reproduced with permission.[98] Copyright 2021, Elsevier. (d) A schematic illustration explains the enhanced electrocatalytic activity and stability of NiPS/NF for water electrolysis in anodic seawater splitting. Reproduced with permission.[70] Copyright 2022, Elsevier. (e) The electrochemical behavior of Ni-LDH, NiFe-LDH, and NiFe-LDH-S350 electrodes was evaluated using linear sweep voltammetry (LSV) measurements in an electrolyte comprising 1.0 M KOH and 0.5 M NaCl. (f) The Tafel slopes of the samples were determined by calculating the slope of the linear portion of the LSV curves. Reproduced with permission.[99] Copyright 2021, Elsevier. (g) Ni_3S_2/Fe–NiP_x/NF and other catalysts with excellent performance, were compared in terms of the overpotentials needed to reach current densities of 100, 500, and 1000 mA cm^{-2} for the OER in 1 M KOH and alkaline natural seawater. Reproduced with permission.[100] Copyright 2022, Wiley-VCH.

bifunctional catalytic performance in simulated seawater electrolyte, with the overpotentials of 174 mV and 365 mV for HER and OER, respectively, at a current density of 100 mA cm^{-2}, and exhibits a stability of more than 120 h at 200 mA cm^{-2} (Fig. 9e–g).

Nickel-based phosphides/sulfides/nitrides can enhance the OER performance by adjusting the proportions and configurations of various elements. Enhancements in catalyst structure optimization, electrocatalytically active site density, electron transfer rate, and surface catalytic activity can greatly improve its OER performance.[107,108] Furthermore, it is essential to thoroughly evaluate and enhance the stability and activity of the catalysts in various settings and circumstances to improve the efficiency of the OER reaction process.

3.1.5 Other nickel-based catalysts. In addition to the catalysts reported above, in recent years researchers have also utilized other methods to modify nickel-based catalysts. Metal-doped nickel-based catalysts have essential application prospects in OER.[109] By doping different metal elements, the electronic structure and surface active sites of the catalysts can be

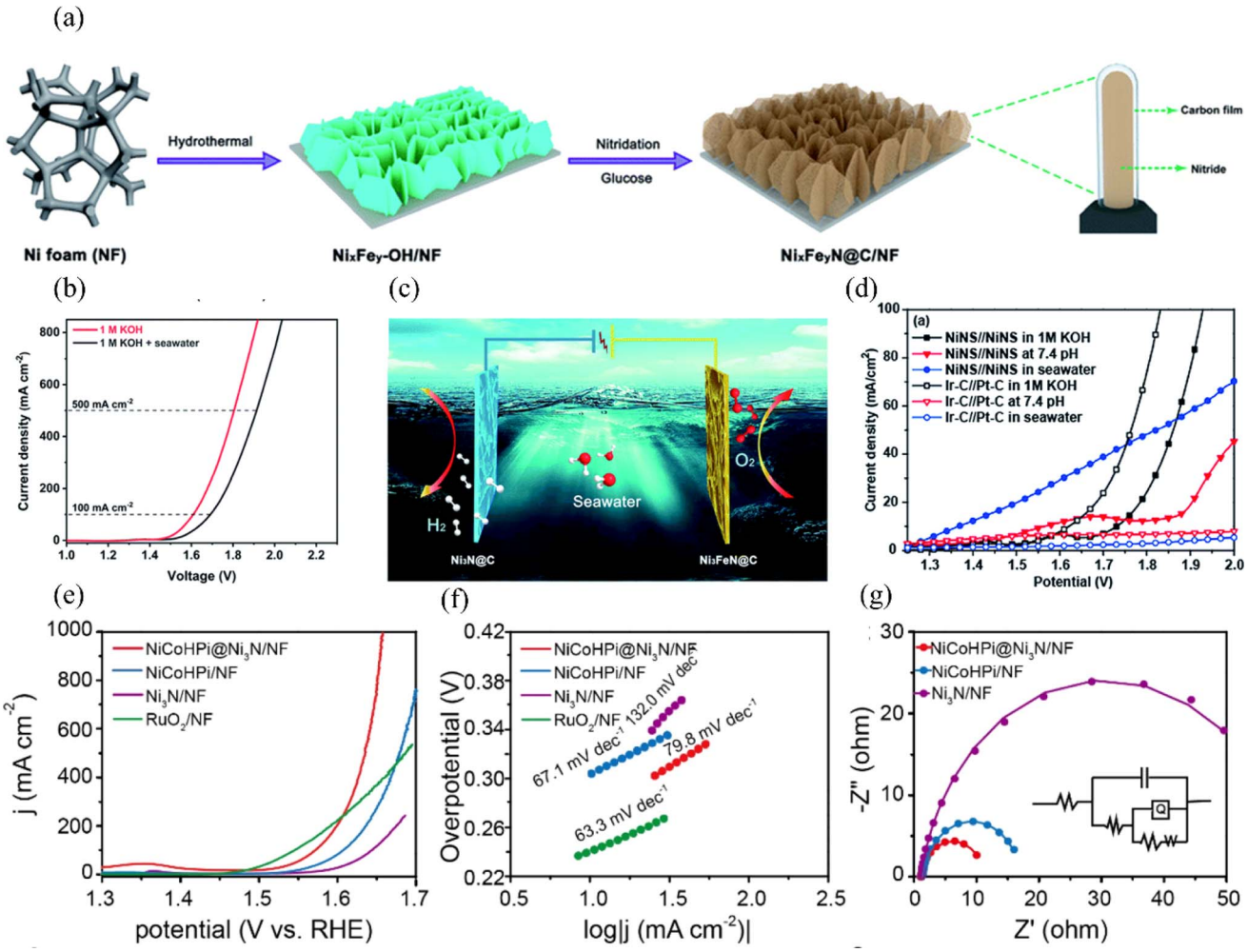

Fig. 9 (a) Synthesis process of Ni_xFe_yN@C/NF. (b) The polarization curves of the electrolyzer were obtained by testing it in electrolytes consisting of 1 M KOH and a mixture of seawater and 1 M KOH. (c) A visual representation of the electrolyzer is depicted, where Ni_3FeN@C/NF is used as the anode and Ni_3N@C/NF serves as the cathode. Reproduced with permission.[103] Copyright 2021, Royal Society of Chemistry. (d) In 1.0 M KOH electrolyte, polarization curves were obtained for the NiNS//NiNS and Ir–C//Pt–C overall water splitting systems. Additionally, polarization curves were also measured in buffer solution with a pH of 7.4 and seawater. Reproduced with permission.[104] Copyright 2019, Royal Society of Chemistry. (e) LSV curves of NiCoHPi@Ni_3N/NF, NiCoHPi/NF, Ni_3N/NF, and Pt/C/NF samples. (f) Tafel plots of NiCoHPi@Ni_3N/NF, NiCoHPi/NF, Ni_3N/NF, and Pt/C/NF samples. (g) Nyquist plots were obtained at a potential of 1.49 V *vs.* RHE for the NiCoHPi@Ni_3N/NF, NiCoHPi/NF, Ni_3N/NF, and Pt/C/NF samples. The polarization curves were also obtained with an 85% *iR* correction. Reproduced with permission.[105] Copyright 2022, Elsevier.

modulated to enhance their catalytic activity and stability. It was discovered that doping extremely small quantities of noble metals can improve the catalyst's intrinsic electronic structure and increase the catalyst's exposure to more active sites.[110] Cui *et al.* synthesized lily-like RuNi–Fe_2O_3/IF catalysts with ultra-low Ru doping using a one-step hydrothermal method, and they found that the appropriate Ru/Ni molar ratio has a significant effect on the formation of lily-like morphology.[67] Meanwhile, the doping of trace noble metal Ru could lead to the exposure of highly active sites on the catalyst surface. Ru doping could also modulate the electronic structure of Ni, which led to the charge redistribution and significantly enhanced the charge number near the Fermi energy. In addition, the applied density of states (DOS) indicates that the DOS of RuNi–Fe_2O_3/IF at the Fermi energy is significantly increased compared to Fe_2O_3, which suggests that more electrons are involved in the catalytic reaction, the conductivity of the catalyst is improved, and the catalytic activity increases. Ultimately, RuNi–Fe_2O_3 achieved an overpotential of only 329.0 mV with a current density of 100 mA cm^{-2}. In addition to doping trace amounts of noble metals, the strategy of bimetallic co-doping can also significantly improve the performance of the electrocatalysts due to the coordinated interactions between the constituent metals.[111] Huang *et al.* designed CoFe–Ni_2P catalysts with layered nanosheet morphology *via* secondary hydrothermal doping of Fe and Co onto nickel phosphide.[112] Fe heteroatoms enhance electrical conductivity, while Co heteroatoms accelerate electrode surface self-reconstruction. It is worth noting that the co-doping of Co and Fe during the synthesis process caused the intermediate product CoFe–$Ni(OH)_2$ to be "melted" after the phosphatization

process, which became a solidifying agent and bonded with the neighboring microchips to form a robust microsphere structure. The layer-by-layer lamellar structure is substantial, which ensures that the CoFe–Ni_2P electrode maintains good solidity and efficient electron transfer during high-current-density electrolysis in seawater environments (Fig. 10a and b). Ultimately, CoFe–Ni_2P requires only a low overpotential of 304 mV to achieve a current density of 500 mA cm^{-2} in a seawater electrolyte of 6 M KOH while operating stably for 600 h.

Ni-based alloy catalysts are highly suitable for OER applications due to their intrinsic polarity arising from the incorporation of different metals. They also boast high mechanical strength, excellent conductivity, and a variety of valence state transitions. Li *et al.* synthesized a high-performance oxygen evolution electrode, NiMoFe/NM, *via* thermal shock, exhibiting excellent OER activity and stability for over 1500 h in simulated alkaline seawater and 550 h in natural seawater.[113] The oxidized NiFeMo electrode forms quickly, and its amorphous surface provides more defect sites, enhancing OER activity (Fig. 10c and d). At the same time, the NiMoFe/NM system reduces the energy barrier of adsorption of translation intermediates (Fig. 10e). In a recent report, Xu *et al.*[114] prepared CoFeLDH@Ni_2P electrocatalysts using cobalt-iron layered double hydroxides and nickel phosphide by hydrothermal and electrodeposition industries. The strong coupling effect between the amorphous cobalt–iron layered double hydroxide interface and the crystalline nickel phosphide interface alters the electronic configuration of the catalyst's active sites. This design approach enhances the electrocatalyst's performance by featuring amorphous–crystalline interfaces. Stability analysis shows the catalyst undergoes unique reconstructive behavior during the OER, forming bimetallic co-precipitated NiOOH (CoFe–NiOOH) and $Ni(OH)_2$,

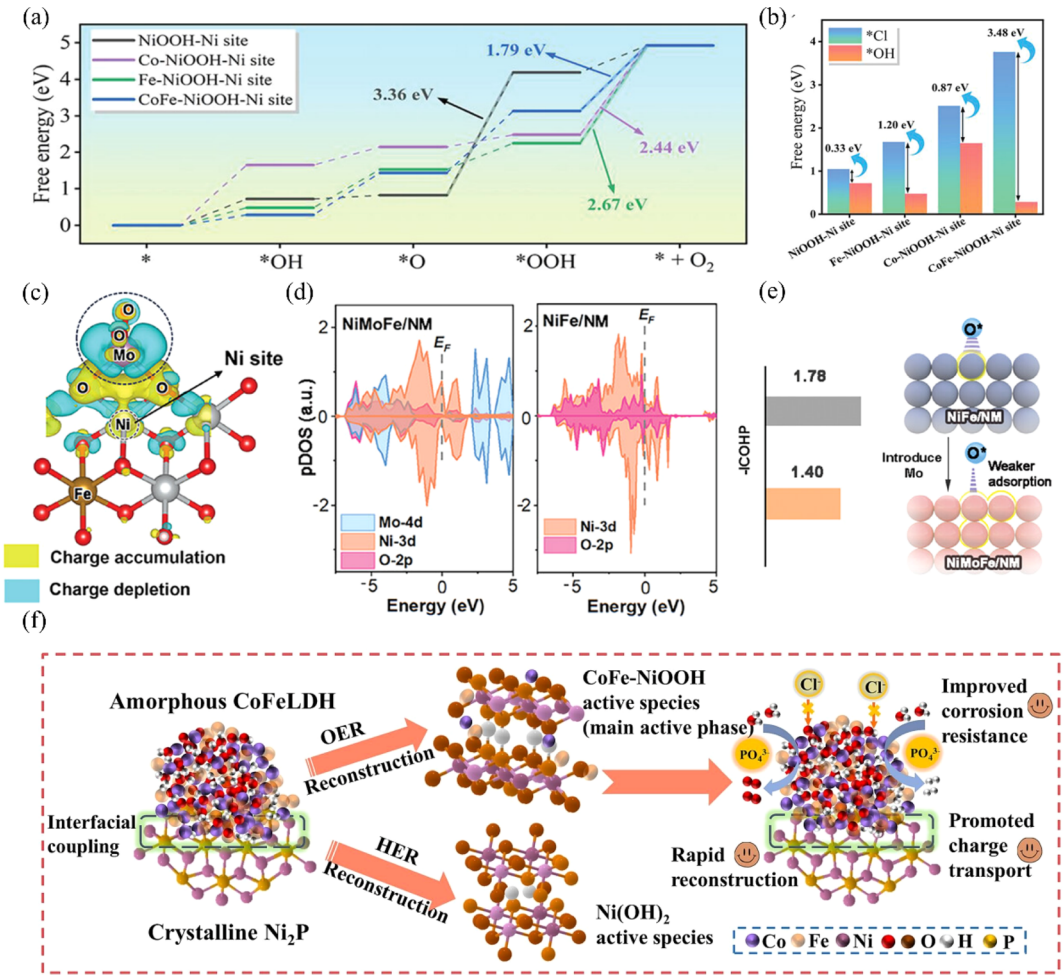

Fig. 10 (a) A reaction energy diagram was constructed to illustrate the OER at the Ni sites on the surface of Ni_2P, Fe–Ni_2P, Co–Ni_2P, and CoFe–Ni_2P materials. (b) The adsorption energies of *Cl and *OH species at the Ni sites on the surfaces of NiOOH, Fe–NiOOH, Co–NiOOH, and CoFe–NiOOH were assessed. Reproduced with permission.[112] Copyright 2023, Elsevier. (c) The charge density difference of γ-(NiFe)OOH after the reformation with MoO_4^{2-} was visualized, where yellow regions indicate electron accumulation and blue regions indicate electron depletion. (d) Visualization of the projected density of states (pDOS) plots for Mo-4d, Ni-3d, and O-2p in the NiMoFe/NM and NiFe/NM systems. (e) The calculated values of the interfacial charge transfer (ICOHP) and a schematic illustration depicting the reduced strength of oxygen-intermediate adsorption in the NiMoFe/NM system. Reproduced with permission.[113] Copyright 2023, Wiley-VCH. (f) The efficient water electrocatalysis activity mechanism diagram, highlighting the roles of CoFeLDH@Ni_2P in the process. Reproduced with permission.[114] Copyright 2024, Elsevier.

Table 1 Performance of recently reported nickel-based OER electrocatalysts

Catalysts	Electrolyte	Overpotential for specific current density	Stability	Ref.
NRAHM-NiO/NF	1.0 M KOH + seawater	340 mV@100 mA cm^{-2}	100 h@500 mA cm^{-2}	75
Fe–NiO_xH_y/CC	1.0 M KOH +0.6 M NaCl	206 mV@10 mA cm^{-2}	12 h@10 mA cm^{-2}	77
NiO_x–FeO_x@g-C_3N_4/NF	1.0 M KOH + seawater	380 mV@1000 mA cm^{-2}	100 h@1000 mA cm^{-2}	79
Ce–NiFe LDH/NF	1.0 M KOH + seawater	390 mV@1000 mA cm^{-2}	500 h@1000 mA cm^{-2}	83
$Mo_{0.25}$–NiFe LDH/NF	1.0 M KOH + seawater	335 mV@500 mA cm^{-2}	500 h@500 mA cm^{-2}	84
NiMoFe/NM	1.0 M KOH + seawater	241 mV@10 mA cm^{-2}	1500 h@100 mA cm^{-2}	113
Fe–Ni_2Pv/NF	1.0 M KOH + seawater	306 mV@1000 mA cm^{-2}	100 h@100 mA cm^{-2}	89
NiO/Ni_3S_2@Ni_5P_4/NF	1.0 M KOH + seawater	310 mV@10 mA cm^{-2}	100 h@100 mA cm^{-2}	90
NiP_x/HA	1.0 M KOH +0.5 M NaCl	392 mV@200 mA cm^{-2}	960 h@500 mA cm^{-2}	94
NiCoS NSAs/NF	1.0 M KOH + seawater	440 mV@500 mA cm^{-2}	100 h@100 mA cm^{-2}	98
NiPS/NF	1.0 M KOH + seawater	392 mV@500 mA cm^{-2}	60 h@200 mA cm^{-2}	70
Ni_3S_2/Fe–NiP_x	1.0 M KOH + seawater	351 mV@1000 mA cm^{-2}	225 h@1000 mA cm^{-2}	100
NiFe-LDH-S	1.0 M KOH +0.5 M NaCl	296 mV@100 mA cm^{-2}	12 h@100 mA cm^{-2}	99
Ni_3FeN@C/NF	1.0 M KOH +0.5 M NaCl	351 mV@500 mA cm^{-2}	100 h@100 mA cm^{-2}	103
NiNS/NF	1.0 M KOH + seawater	404 mV@100 mA cm^{-2}	12 h@100 mA cm^{-2}	104
NiCoHPi@Ni_3N/NF	1.0 M KOH + seawater	396 mV@100 mA cm^{-2}	120 h@200 mA cm^{-2}	105
RuNi–Fe_2O_3/IF	1.0 M KOH + seawater	497 mV@1000 mA cm^{-2}	100 h@100 mA cm^{-2}	67
CoFe–Ni_2P/NF	6.0 M KOH + seawater	304 mV@500 mA cm^{-2}	600 h@500 mA cm^{-2}	112
CoFeLDH@Ni_2P/NF	1.0 M KOH +0.5 M NaCl	363 mV@100 mA cm^{-2}	55 h@100 mA cm^{-2}	114

which enhance OER activity and corrosion resistance (Fig. 10f). The catalyst requires a lower overpotential of 398 mV to achieve a current density of 100 mA cm^{-2} in alkaline seawater electrolyte, surpassing most reported nickel-based materials (Table 1).

3.2 Nickel-based catalysts for HER

For the HER, Ni has the smallest $|\Delta G_{H^*}|$ among all transition metals, the ability to reach the maximum current density at the same overpotential, and the ability to tune the electronic configuration of the surrounding elements, which contributes to the enhancement of the HER activity.[69,115] Researchers have modified nickel-based materials by defect engineering and elemental doping to construct efficient nickel-based HER catalysts. This section summarizes the HER catalysts reported in recent years at home and abroad.

3.2.1 Nickel-based catalysts with noble metal traces. It was found that the doping of small amounts of noble metals can improve the performance of catalysts in several ways compared to non-precious metal catalysts.[116] Firstly, small quantities of precious metal doping improved the surface structure of the catalysts and increased the number of active sites on their surfaces. This enables the catalyst to provide more effective reaction sites, thus enhancing the reaction activity.[117] Secondly, doping with a small amount of noble metals enhances the electron arrangement and transport properties on the catalyst surface. This modulation of the electronic structure increases the adsorption and electron transfer rate of reactants, thereby promoting the catalytic reaction.[110,118] Therefore, doping small amounts of precious metals play an essential role in enhancing catalytic activity and promoting HER.[119] Through the combined effect of these mechanisms, precious metal doping can exert its unique catalytic properties, providing new strategies and solutions for efficient energy conversion and storage. Using this strategy, Zhai *et al.* doped a small amount of Ir onto a nickel–iron-based MOF substrate with a high specific surface area using a one-step hydrothermal method, resulting in MIL-(IrNiFe)@NF (Fig. 11b).[120] The tri-metal synergy significantly increased the active sites on the catalyst surface, enhancing its overall catalytic performance. The addition of Ir induces the formation of a unique microsphere structure on the catalyst surface, while the MOF structure enhances ion diffusion paths. Additionally, the nickel foam substrate increases the surface's electrical conductivity, further improving the catalyst's performance. Combined with the above reasons, the MOFs (MIL-(IrNiFe)@NF) have excellent HER catalytic activity as well as corrosion resistance in alkaline seawater electrolytes. It only requires 235 mV to catalyze the HER to reach a current density of 1000 mA cm^{-2} in alkaline natural seawater (Fig. 11a). Hu *et al.* prepared Pt–Ni@NiMoN by ammonolysis after embedding and loading a very low amount of Pt (0.07 wt%) onto transition metal nitride (NiMoN) carriers (Fig. 11c).[121] This resulted in Pt–Ni@NiMoN exhibiting superior HER catalytic properties compared to commercially available 20 wt% Pt/C electrocatalysts. Due to the strong inter-electronic interactions between Pt and other atoms and enhanced water polarization, the catalyst has an overpotential of only 90 mV in seawater up to a current density of 500 mA cm^{-2} and remains stable for more than 200 h in a highly concentrated (2 M) seawater sodium chloride solution, which has the potential to be used in large-scale industrial applications (Fig. 11d and e). Based on a similar strategy, Su *et al.* combined ultra-low-content Pt with substable-phase hexagonal close-packed Ni to prepare Pt-hcp Ni NBs (Fig. 11f), whose unique crystal structure optimizes the adsorption process of the reaction intermediates, with an overpotential of 137 mV at 10 mA cm^{-2} in real seawater electrolysis.[122] Although the doping of trace precious metals will improve the activity of nickel-based catalysts, due to the scarcity and high cost of precious metals, gradually finding methods to

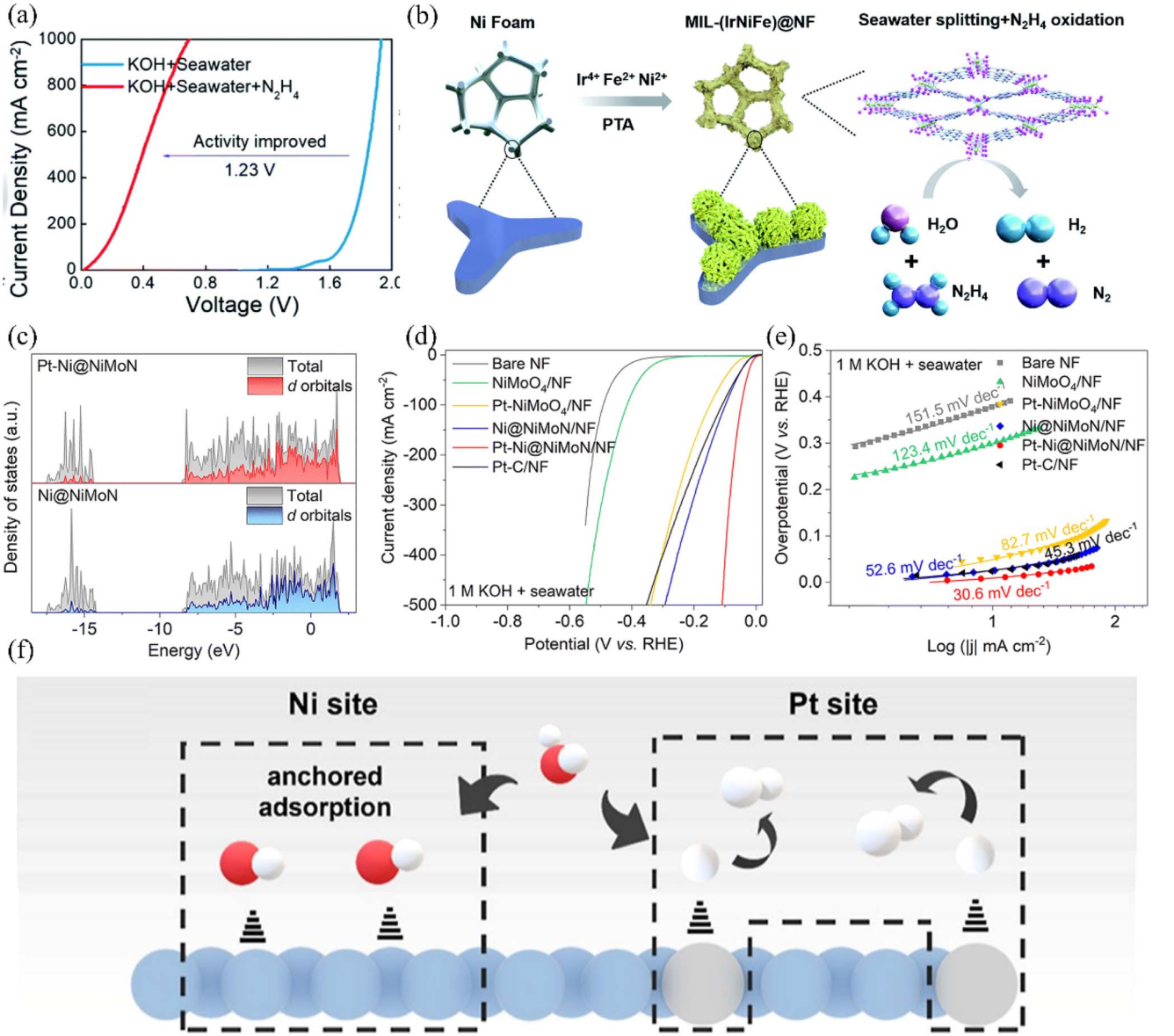

Fig. 11 (a) Comparison of the OER polarization curves for the electrolyzer containing MIL-(IrNiFe)@NF catalyst in two different electrolyte conditions: 1.0 M KOH + seawater and 1.0 M KOH + seawater + 0.5 M N_2H_4. (b) Illustrative diagram depicting the step-by-step formation process of the MIL-(IrNiFe)@NF catalyst. Reproduced with permission.[120] Copyright 2021, Royal Society of Chemistry. (c) Calculated DOS for Ni@NiMoN and Pt–Ni@NiMoN. Bare NF, $NiMoO_4$/NF, Pt–$NiMoO_4$/NF, Ni@NiMoN/NF, Pt–Ni@NiMoN/NF and Pt–C/NF in 1 M KOH + real seawater. (d) The LSV curves. (e) The Tafel plots. Reproduced with permission.[121] Copyright 2023, Royal Society of Chemistry. (f) Enlarged view of Ni sites and the Pt site mechanism in the reaction. Reproduced with permission.[122] Copyright 2023, American Chemical Society.

replace the doping of trace precious metals will be a future research direction.

3.2.2 Nickel-based catalysts with non-precious metal doping. The doping strategy of non-precious metal elements shows apparent advantages in catalyzing the HER in seawater electrolysis. Firstly, compared with the doping of trace precious metals, the direct doping of inexpensive metals can further reduce the cost of catalyst preparation, which is conducive to the realization of large-scale industrial applications.[123] Secondly, introducing transition metals, for example, can introduce additional active sites for nickel-based catalysts and modulate the surface and electronic structures of catalysts.[124] Finally, the introduction of some metal elements can reduce the ΔG_{H^*} and also accelerate the desorption of OH*, which results in the rapid release of active sites, thus accelerating the kinetics of the HER.[125] Lu *et al.* synthesized Mn–NiO–Ni/Ni–F by pyrolyzing manganese-based metal–organic frameworks (Mn-MOF) on nickel foam.[126] The Mn-doped Mn–NiO–Ni/Ni–F demonstrated superior catalytic performance compared to the pristine NiO–Ni composite, as the presence of Mn decreased the ΔG_{H^*}, enhancing catalytic activity for HER (Fig. 12a). Additionally, the presence of Mn was found to enhance the catalytic stability of NiO–Ni composites. This improvement is attributed to the formation of $NiMnO_x$ on the catalyst surface, which protects the

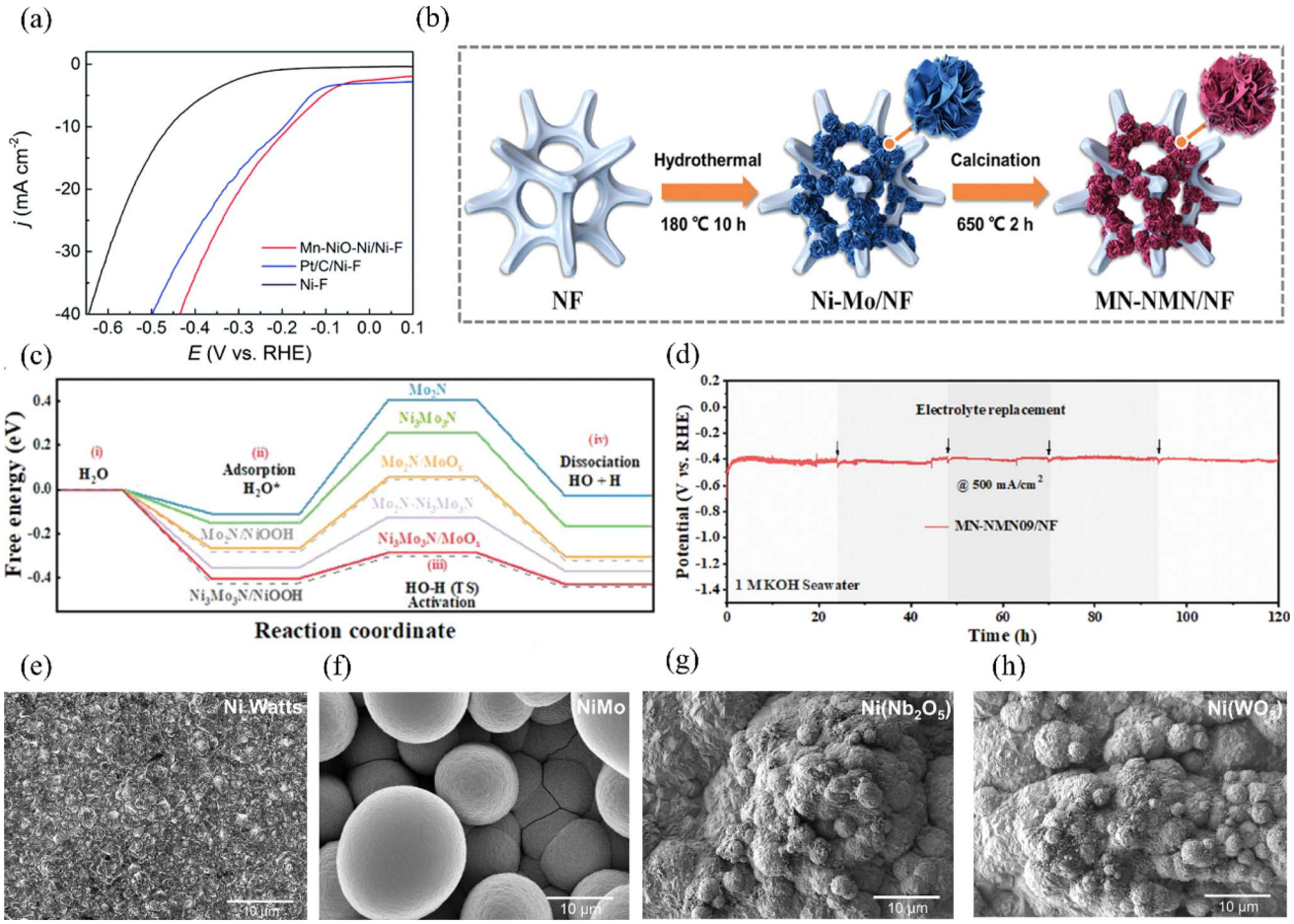

Fig. 12 (a) The LSV curves of Mn–NiO–Ni/Ni–F, Pt/C/Ni–F and Ni–F in natural seawater. Reproduced with permission.[126] Copyright 2018, Royal Society of Chemistry. (b) Schematic depiction of the synthetic pathways employed for the fabrication of MN-NMN-based catalysts. (c) A computed free energy diagram showcasing the energetics of H_2O*, H–OH, and [H + OH]* on various catalysts, including Mo_2N, Ni_3Mo_3N, Mo_2N/MoO_x, Mo_2N–Ni_3Mo_3N, Ni_3Mo_3N/MoO_x, Mo_2N/NiOOH, and Ni_3Mo_3N/NiOOH. (d) Stability tests of MN-NMN09/NF were conducted using chronoamperometry, maintaining constant current densities of 500 mA cm^{-2} for 120 hours in an alkaline seawater electrolyte. Reproduced with permission.[127] Copyright 2023, Wiley-VCH. Scanning electron micrographics of the (e) Ni-Watts. (f) NiMo alloy. (g) Ni(Nb_2O_5) composite. (h) Ni(WO_3) composite. Reproduced with permission.[128] Copyright 2022, Elsevier.

outer layer from oxidation. As a result, the catalytic activity remains stable for hundreds of hours during the HER. In the electrolysis of natural seawater test, the catalyst showed superior HER catalytic performance to Pt/C with lower onset overpotential. To investigate strategies for enhancing the HER activity and stability of nickel-based materials through elemental doping, Ysea *et al.* compared NiMo alloy catalysts, Ni(WO_3), and Ni(Nb_2O_5) composite catalysts with pure nickel-based catalysts (Fig. 12e–h).[128] They found that all doped catalysts, unlike the pure nickel-based ones, exhibited irregular surface areas, which increased the number of active sites and surface roughness, thereby improving catalytic activity. It was found that NiMo alloys have higher solubility under corrosive conditions, while nickel matrix composites exhibit better corrosion resistance. This is due to the higher proportion of (111) nickel planes compared to (200) planes, resulting in lower surface energy. The higher $I_{(111)}/I_{(200)}$ ratio indicates better stability of the catalysts. Therefore, composites are superior to single Mo-doped catalysts, which is conducive to improving the stability of nickel-based materials in future hydrogen production from electrolytic seawater. Therefore, the use of composites is superior to single Mo-doped catalysts, which is conducive to improving the stability of nickel-based materials in future hydrogen production from electrolytic seawater. Furthermore, NiMo-based alloys have been found to bring the ΔG_{H^*} in the HER close to zero. Based on this, Zhu *et al.* synthesized heterogeneous Mo_2N/Ni_3Mo_3N electrocatalysts (Fig. 12b).[127] They achieved this by optimizing the ratio of NiMo-based content on a nickel foam substrate and calcining the precursor with the determined optimum molybdenum content under ammonia gas. The electrocatalyst can reach a current density of 500 mA cm^{-2} in seawater electrolyte at a low overpotential of 123 mV for HER and has a stability of more than 120 h (Fig. 12d). According to Raman analysis, the catalyst can adsorb H_2O faster and dissociate OH^- faster in the HER, and DFT disclosed that the heterogeneous interfacial structure can reduce the ΔG_{H^*} of the catalyst (Fig. 12c). Bu *et al.* utilized the property that NiMo-based alloys can reduce ΔG_{H^*} and prepared

$NiMo@C_3N_5$ catalysts with a unique heterogeneous structure by using two-dimensional C_3N_5 as a shell.[129] The carbon-based shell effectively protects the catalyst's inner core from seawater poisoning and optimizes the HER pathway. Density functional theory calculations revealed multiple electron transport channels at the interface between the NiMo inner core and the carbon-based shell. This "killing two birds with one stone" property lowers the reaction rate step's energy barrier and reduces the reaction's overpotential. Finally, $NiMo@C_3N_5$ Faraday efficiency in seawater was as high as 94.8%. These aforementioned reports suggest that the development of high-performance HER electrocatalysts by doping and interfacial engineering of non-precious metal elements is a feasible strategy.

Non-precious metal-doped nickel-based electrocatalysts can be used in various methods to enhance the efficiency of HER in diluted seawater. Key efforts include optimizing the structural design of catalysts and managing lattice defects to boost active site density and enhance electron transport rate. Furthermore, the catalytic activity of HER can be improved through surface modification and the inclusion of appropriate heteroatoms or chemicals. When conducting HER in seawater, it is important to evaluate the stability of the catalyst and its capacity to resist contaminants in saltwater to guarantee the catalyst maintains efficient and durable performance in challenging conditions.

3.2.3 Nickel-based phosphide. In addition to enhancing the intrinsic activity of the OER, nickel-based phosphides also play a crucial role in boosting the intrinsic activity of the reaction during the synthesis of HER catalysts.[130] Nickel-based

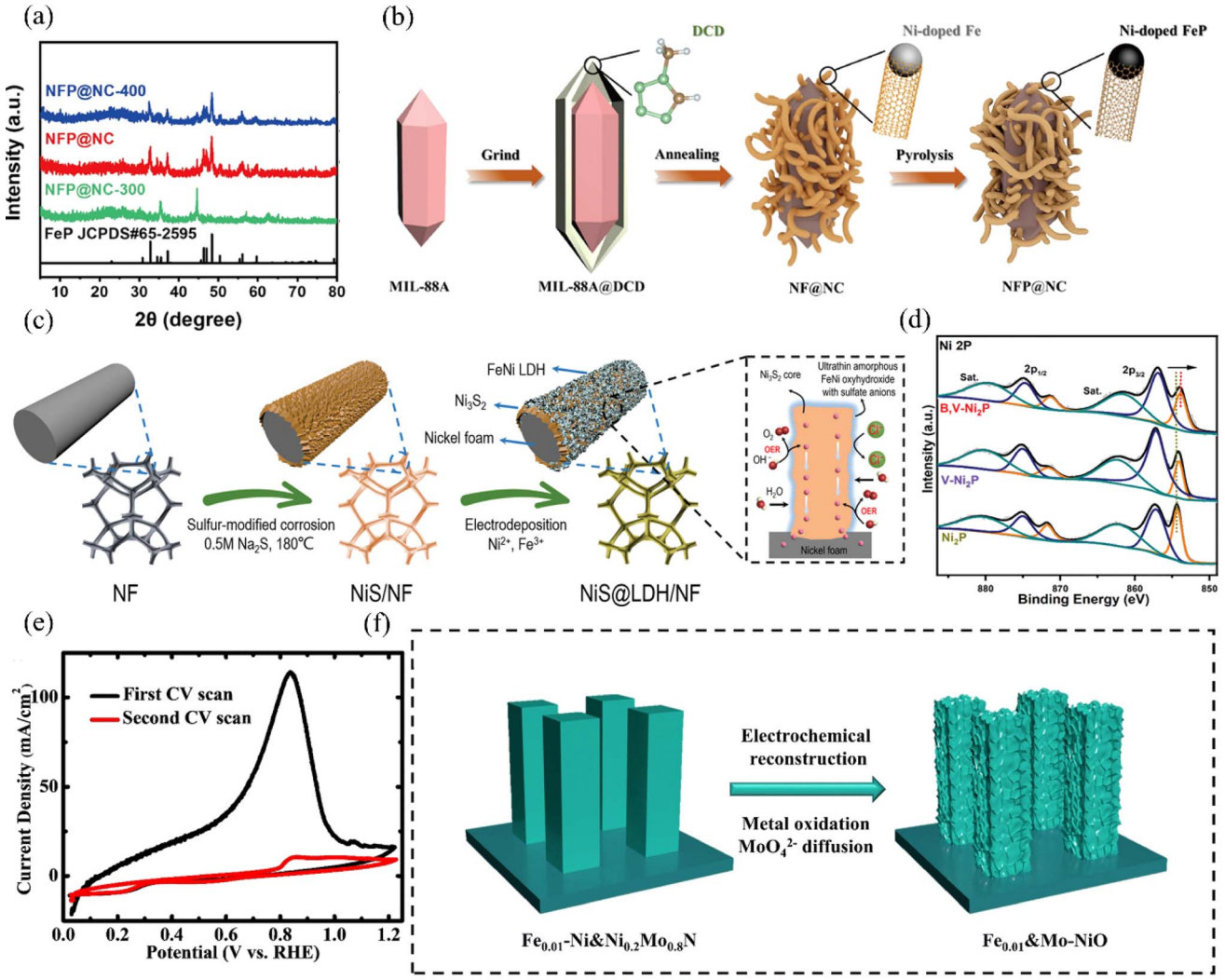

Fig. 13 (a) XRD patterns of NFP@NC-300, NFP@NC, and NFP@NC-400 were analyzed. (b) Schematic illustration of the synthesis process of the NFP@NC. Reproduced with permission.[131] Copyright 2023, Springer Nature. (c) Schematic illustration of the synthesis of core–shell-structured NiS@LDH/NF. Reproduced with permission.[132] Copyright 2023, Wiley-VCH. (d) XPS spectra of Ni 2p were obtained for B,V-Ni_2P, V-Ni_2P, and Ni_2P. Reproduced with permission.[133] Copyright 2023, Wiley-VCH. (e) Electrochemical reconstruction of $Fe_{0.01}$–Ni&$Ni_{0.2}Mo_{0.8}N$ was observed by cyclic voltammetry (CV) scans. (f) A schematic representation of the electrochemical reconstruction process of $Fe_{0.01}$–Ni&$Ni_{0.2}Mo_{0.8}N$, transforming into $Fe_{0.01}$&Mo–NiO, is depicted. Reproduced with permission.[48] Copyright 2022, Royal Society of Chemistry.

phosphides increase the catalysts' activity and stability and offer abundant active sites for reactant adsorption and electron transfer, as illustrated in Fig. 13a and b.[131] Moreover, their excellent chemical stability and corrosion resistance enable them to maintain high activity and longevity throughout extended reaction processes. Furthermore, the rich tunability of nickel-based phosphides allows for precise adjustment of catalyst activity and selectivity by modulating synthesis methods, composition, and structure.[70] This tunability enhances the flexibility and options available for catalyst design and optimization.

Nickel phosphide has garnered attention among recent HER electrocatalysts for its high electrical conductivity, activity, and tunable electronic configuration. The phosphate layer formed by surface oxidation in seawater repels Cl^- ions and mitigates catalyst corrosion effectively.[134] Zhao *et al.* synthesized a B,V-Ni_2P electrode by co-doping boron and vanadium phosphide. Vanadium doping enhances the dissociation of water by nickel phosphide, while boron and vanadium co-doping adjusts the electronic configuration of nickel phosphide, promoting interaction with intermediate products and enhancing HER activity.[133] In addition, the doping of V also favours the induction of Ni lattice distortion, and according to XPS, the Ni_2P binding energy is negatively shifted (Fig. 13d), indicating that its electrons undergo rearrangement. Ultimately, the B,V-Ni_2P electrocatalysts only require an overpotential of 162 mV to reach a current density of 100 mA cm^{-2} in the simulated seawater of 1 M KOH and 0.5 M NaCl, and the nanomorphology of the surfaces has also remained essentially. The nanomorphology of its surface was also basically unchanged in the long-term test, which has good stability.

3.2.4 Nickel-based sulfides. Similar to nickel phosphides, nickel sulfides also exhibit high chemical stability in seawater electrolysis environments, particularly in chloride-containing seawater where they demonstrate superior corrosion resistance.[135] Furthermore, nickel sulfides typically present lower overpotentials in HER, thereby enhancing the efficiency of the HER process.[119] This combination of high chemical stability and low overpotential makes nickel sulfides highly effective catalysts for HER in seawater electrolysis.

Ren *et al.* utilized nickel sulfide (Ni_3S_2) on nickel foam to design the heterostructure NiS@LDH/NF with OER activity.[132] They then phosphorylated it to obtain NiS@FeNiP/NF, which exhibited excellent HER activity (Fig. 13c). During the synthesis, electron transfer from Ni_3S_2 to the $FeNi_2P$ interface facilitated charge redistribution, improving interaction with reaction intermediates. Consequently, the HER activity in alkaline seawater electrolyte was significantly enhanced compared to NiS@LDH/NF. Through a combination of theoretical calculations and experiments, researchers found that NiS@FeNiP/NF, with its superhydrophobic/superhydrophilic surface properties, exhibits excellent H_2O adsorption capacity and promotes hydrogen release during the HER. This enables the catalyst to reach 500 mA cm^{-2} in an alkaline seawater electrolyte, with an overpotential of 237 mV. Fan *et al.* developed a heterogeneous and corrosion-resistant iron–sulfur-based catalytic electrode, NiS–FeS@IF, using a simplified one-step sulfuration-etching method.[135] This catalyst demonstrated a low overpotential of just 322 mV for the HER at a current density of 500 mA cm^{-2}. More importantly, the NiS–FeS@IF electrode sustained industrial-grade high current densities of 1 A cm^{-2} for over 500 h without significant performance degradation. The distinct and evenly distributed structure of NiS–FeS improves interfacial electron transfer, maximizes the exposure of active sites, and offers efficient routes for quick bubble release and mass transfer. Additionally, this straightforward one-step sulfuration method, distinct from traditional hydrothermal methods, shows promise for large-scale industrial production.

3.2.5 Nickel-based nitrides. Nickel nitrides, while having lower intrinsic catalytic activity and fewer active sites compared to nickel phosphides and sulfides, offer significant advantages as electrocatalysts for HER. They exhibit excellent mechanical strength and chemical stability, maintaining structural integrity during prolonged operation. Their good corrosion resistance in seawater electrolysis environments enables them to withstand chloride ion corrosion effectively.[136] Additionally, nickel nitrides are cost-effective and possess good electrical conductivity, enhancing electron transfer efficiency. Their multifunctionality allows for performance optimization through element doping, adjusting their electronic structure and catalytic properties.[138,139] Despite their lower intrinsic activity, these strengths make nickel nitrides promising candidates for HER electrocatalysis.

Table 2 Performance of recently reported nickel-based HER electrocatalysts

Catalysts	Electrolyte	Over potential for specific current density	Stability	Ref.
MIL-(IrNiFe)/NF	1.0 M KOH + seawater	235 mV@1000 mA cm^{-2}	100 h@100 mA cm^{-2}	120
Pt–Ni@NiMoN/NF	1.0 M KOH + seawater	11 mV@10 mA cm^{-2}	110 h@400 mA cm^{-2}	121
Pt-hcp Ni NBs	1.0 M KOH + seawater	137 mV@10 mA cm^{-2}	130 h@500 mA cm^{-2}	122
MN-NMN/NF	1.0 M KOH + seawater	123 mV@500 mA cm^{-2}	120 h@500 mA cm^{-2}	126
NiMo@C_3N_5	pH = 7.4 seawater	486 mV@10 mA cm^{-2}	10 h@10 mA cm^{-2}	129
NiS@FeNiP/NF	1.0 M KOH + seawater	327 mV@1000 mA cm^{-2}	120 h@500 mA cm^{-2}	132
Fe_x–Ni&$Ni_{0.2}Mo_{0.8}N$/NF	1.0 M KOH + seawater	69 mV@100 mA cm^{-2}	80 h@425 mA cm^{-2}	48
B,V-Ni_2P	1.0 M KOH +0.5 M NaCl	162 mV@100 mA cm^{-2}	100 h@500 mA cm^{-2}	133
NiS–FeS@IF	1.0 M KOH +0.5 M NaCl	322 mV@500 mA cm^{-2}	500 h@1 A cm^{-2}	136
Ni-SN@C	1.0 M KOH + seawater	23 mV@10 mA cm^{-2}	24 h@10 mA cm^{-2}	137

Based on the property that NiMo-based alloys can reduce ΔG_{H^*}, Ning *et al.* successfully synthesized Fe-doped NiMo-based alloy nitrides Fe_x–Ni&$Ni_{0.2}Mo_{0.8}N$ on nickel foam.[48] These catalysts exhibited excellent HER activity, achieving efficiencies comparable to the highest among reported non-precious metal catalysts. Meanwhile, they found that varying the doping concentration of Fe element can change the nanorod size in the catalyst on the one hand. On the other hand, it will significantly affect its intrinsic HER activity. It is found that C_{dl} decreases with the increase of Fe doping, which indicates that the increase of Fe doping leads to the decrease of ECSA. In contrast, a small amount of Fe doping does not change the intrinsic activity of the catalyst, and also its electrochemically reconstructed product $Fe_{0.01}$&Mo–NiO exhibits superior OER performance (Fig. 13e and f). Jin *et al.* developed a catalyst featuring abundant unsaturated Ni–N bonds, designated as Ni-SN@C, for the HER in alkaline seawater.[136] This catalyst exhibited both high activity and stability, achieving a remarkably low overpotential of 23 mV at a current density of 10 mA cm^{-2}, outperforming commercial Pt/C. Moreover, Ni-SN@C demonstrated the ability to generate hydronium ions in high-pH electrolytes, a characteristic similar to that of precious metal catalyst Pt. This study underscores the significant potential of surface modification engineering of transition metals for industrial hydrogen production (Table 2).

4. Anti-corrosion strategies for nickel-based materials

In contrast to freshwater electrolysis, seawater electrolysis faces electrode corrosion due to the corrosive nature of chloride ions

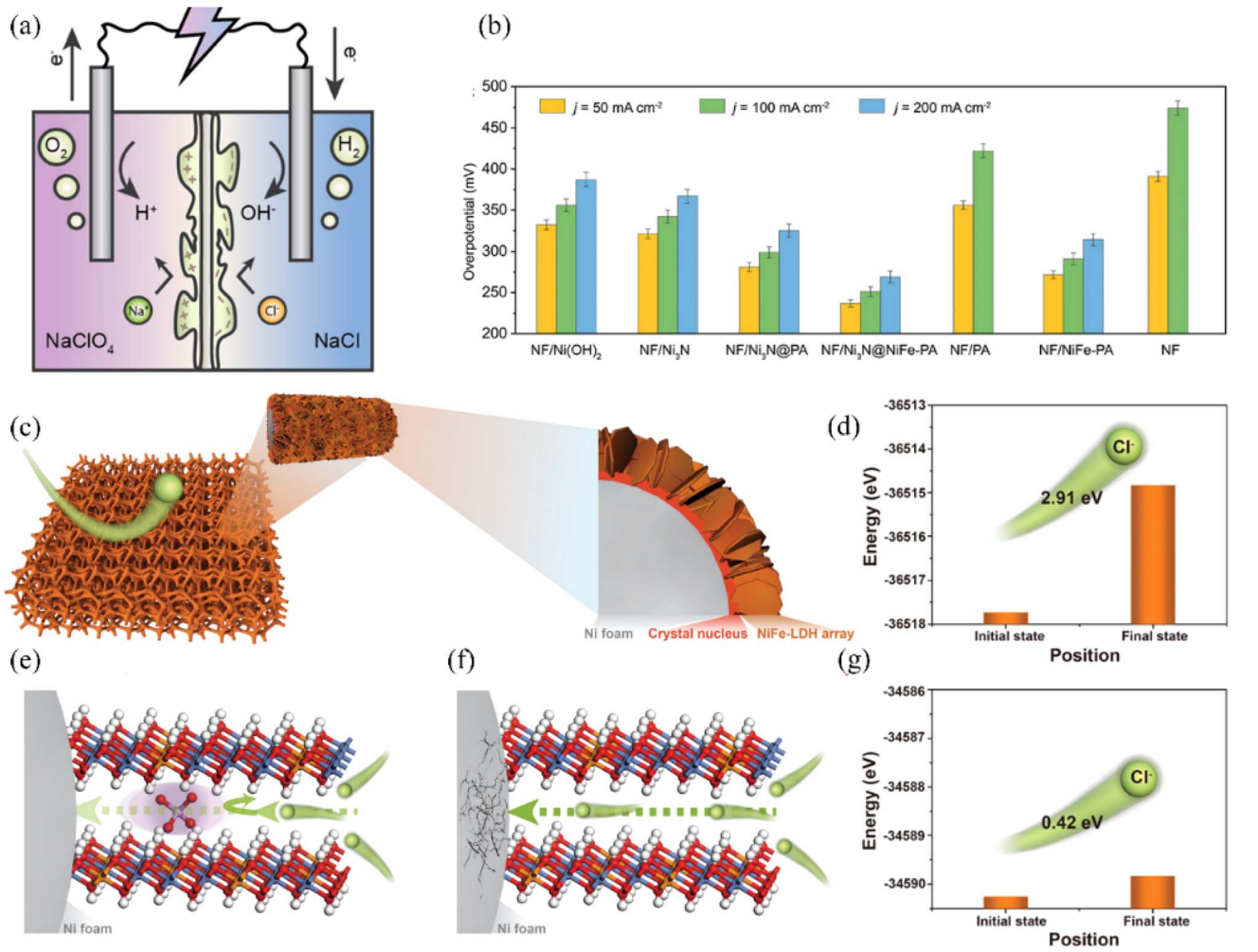

Fig. 14 (a) A visual representation is provided to demonstrate the implementation of double-polyamide thin-film composite (TFC) membranes in seawater electrolysis. Reproduced with permission.[144] Copyright 2024, American Chemical Society. (b) The electrocatalytic performance for the OER of different samples, including NF, NF/Ni(OH)$_2$, NF/Ni_3N, NF/Ni_3N@PA, NF/Ni_3N@NiFe-PA, NF/PA, and NF/NiFe-PA, has been evaluated in alkaline simulated seawater (1 M KOH + 0.5 M NaCl). A summary of the overpotentials required for achieving current densities of 50, 100, and 200 mA cm^{-2} for each sample is provided. Reproduced with permission.[145] Copyright 2023, Wiley-VCH. (c) The structure of NiFe-LDH supported on Ni foam can be visually depicted through a schematic illustration. (d) Energetic barriers to Cl^- migration in PO_4^{3-}/NiFe-LDH. (e) Schematic representation of PO_4^{3-} against Cl^- corrosion in PO_4^{3-}/NiFe-LDH environment. (f) Schematic representation of Cl^- crossing NiFe-LDH without any ionic intercalation. (g) Energy barrier for Cl^- migration in NiFe-LDH without ionic intercalation. Reproduced with permission.[146] Copyright 2022, Wiley-VCH.

present in seawater. Researchers have explored various strategies to enhance the stability and prolong the service life of nickel-based materials in this challenging environment.[35,140] Apart from leveraging the inherent corrosion resistance of nickel-based materials, efforts have been made to target the development of high-activity catalysts for seawater electrolysis at low overpotential conditions, focusing on improving OER selectivity and reducing the competitive CER.[141] Recent studies have concentrated on enhancing the corrosion resistance of nickel-based electrocatalyst materials through doping with corrosion-resistant ions, utilizing electrostatic repulsion, and incorporating protective layers.[142,143]

4.1 Electrostatic repulsion strategy

Construction of polyanionic systems on catalyst surfaces or intercalations, shielding the corrosive effect of chloride ions by electrostatic repulsion and thus increasing the stability of the catalyst is a common corrosion resistance strategy (Fig. 14a).[144,147] Zhang *et al.* investigated the impediment to Cl^- migration using different ionic intercalations between NiFe-LDH intercalations through DFT calculations (Fig. 14c).[146] The results showed that the PO_4^{3-} intercalation had the strongest rejection of chloride ions, where the migration energy barrier of chloride ions was 2.91 eV (Fig. 14d), which was higher than that of its control CO_3^{2-} (2.57 eV) and OH^- intercalation (0.86 eV). As a result, a strategy to intercalate PO_4^{3-} groups in NiFe-LDH is proposed, where PO_4^{3-} carrying a large negative charge can facilitate an electrostatic repulsion strategy to prevent chloride ions from passing through the NiFe-LDH intercalation, preventing the nickel matrix from being corroded (Fig. 14e–g). A series of electrochemical tests revealed that the corrosion resistance life of PO_4^{3-} inserted NiFe-LDH was extended by

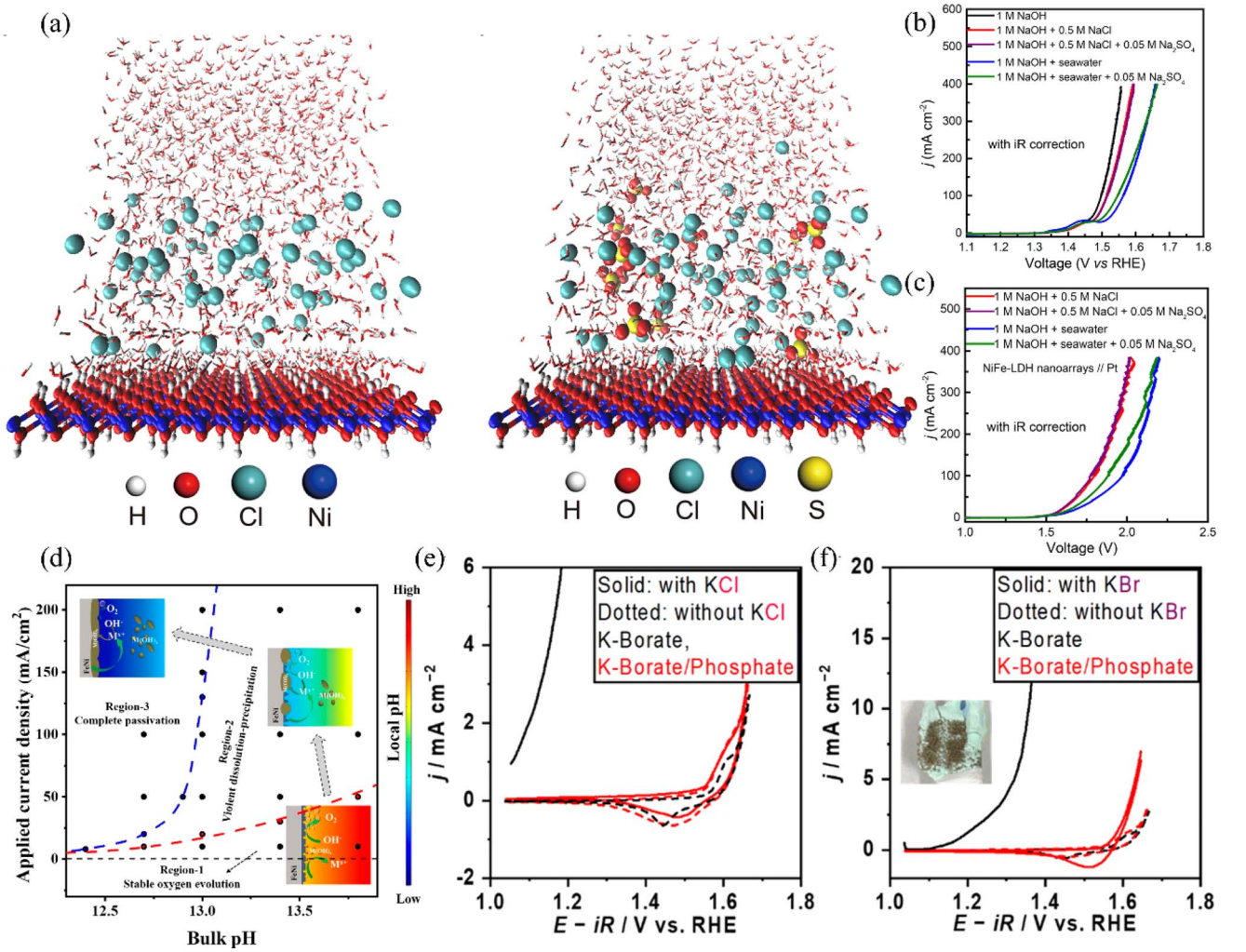

Fig. 15 (a) Visual representations of electrolyte systems above the electrode surface obtained from classical molecular dynamics simulations. (b) Comparison of the electrochemical performance for OER on NiFe-LDH nanoarrays supported on NF in electrolytes with and without SO_4^{2-}, presented as LSV curves. (c) In different electrolytes, the LSV curves of NiFe-LDH/NF with *iR* compensation for overall water splitting are obtained. Reproduced with permission.[150] Copyright 2021, Wiley-VCH. (d) The figure is a schematic representation of the degradation behaviour of the model electrode at different local pH values. Reproduced with permission.[151] Copyright 2024, American Chemical Society. (e) CV curves of $NiFeO_x$ in K-borate and K-borate/phosphate electrolytes in KCl. (f) CV curves of $NiFeO_x$ in K-borate and K-borate/phosphate electrolytes in KBr.[152] Copyright 2024, Royal Society of Chemistry.

more than one hundred times compared to pristine NiFe-LDH. Based on the same principle, NF/Ni_3N@NiFe-PA constructed by Li *et al.* also has good corrosion resistance. The researchers quantified the concentration of Cl^- by ion chromatography, and NF/Ni_3N@NiFe-PA only adsorbed 0.11 mm Cl^-, which is lower than the original NF/Ni_3N (0.26 mm Cl^-) (Fig. 14b).[145] The phosphate-rich surface of the catalyst prevents chloride ion corrosion through electrostatic repulsion. Additionally, the multilayer structure of corrosion-resistant Ni_3N and *in situ*-generated NiFeOOH enhances corrosion inhibition. Besides phosphate groups, sulfur-containing, carbon-containing, and other anionic groups are also used to improve corrosion resistance based on electrostatic repulsion principle.[99,148] Kang *et al.* reported a RuMoNi electrocatalyst with *in situ*-grown $MoSO_4^{2-}$ that preferentially adsorbs at the anode and repels chloride ions during electrolysis, which can be operated continuously for 3000 h at a current density of 500 mA cm^{-2} and is 100% selective for OER in a 1 M KOH + simulated seawater electrolyte.[38]

4.2 Adding corrosion inhibitors to the electrolyte

The addition of corrosion inhibitors to the electrolyte can serve two main purposes: promoting the exclusion of chloride ions by the polyanion in the electrolyte or facilitating a reaction between a specific component in the electrolyte and the catalyst surface.[149] This reaction can lead to forming a passivation layer on the catalyst surface, thereby enhancing its corrosion resistance. Ma *et al.* exploited this strategy by adding sulphate to the electrolyte to improve catalyst corrosion resistance, and the catalysts were stable for 3–5 times longer than when reacting in a seawater electrolyte without SO_4^{2-} (Fig. 15a–c).[150] Recently, Hiroki *et al.*[152] added a borate/phosphate hybrid additive to an alkaline seawater electrolyte, where borate is used as a buffering reagent to maintain the stability of the electrolyte pH. In contrast, phosphate can form a passivation layer with Ni on the catalyst at a pH of 9.2, preventing the catalyst from dissolving due to corrosion (Fig. 15e and f). Researchers used redox probes and *Operando* XAS analysis to investigate the catalyst's corrosion protection mechanism at non-extreme pH levels. They ruled out electrostatic repulsion as

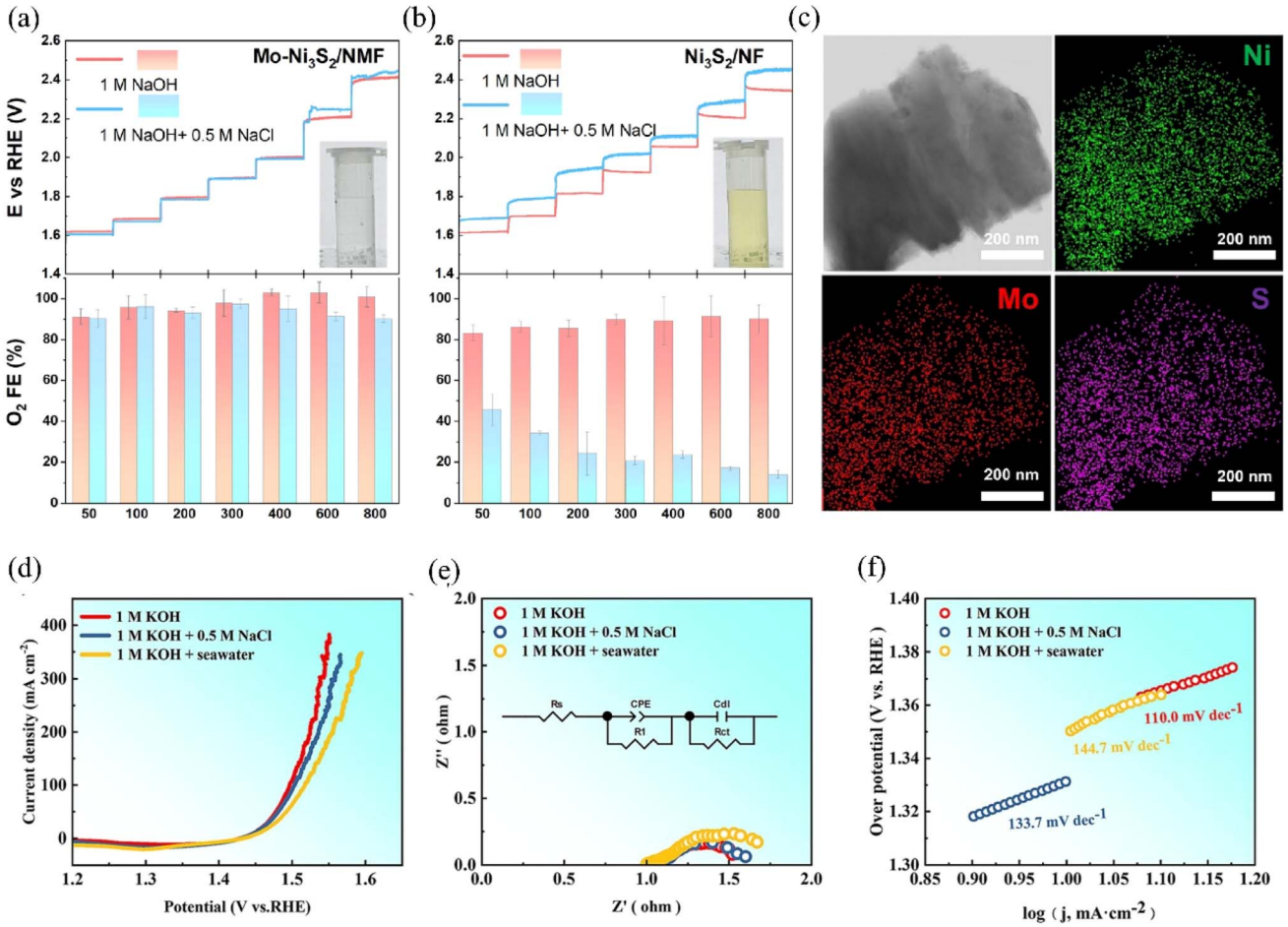

Fig. 16 Anodic activity CP tests without *iR* compensation and corresponding O_2 Faraday electrical efficiency measurements were performed on (a) Mo–Ni_3S_2/NMF and (b) Ni_3S_2/NF in N_2-saturated 1.0 M NaOH electrolytes containing 0.5 M NaCl and no NaCl, respectively, at currents from 50 to 800 mA. The hold time for each step was set to 300 s. The inset in the figure shows a photograph of the electrolyte after iodide titration. (c) The HAADF-STEM image and elemental mapping of Mo–Ni_3S_2/NMF are shown. Reproduced with permission.[157] Copyright 2023, Elsevier. OER performance of HEA-NCFCC/NF@EA in 1.0 M KOH, 1.0M KOH + 0.5 M NaCl and alkaline seawater (d) polarization curves; (e) electrochemical impedance spectroscopy; (f) Tafel plots;[158] Copyright 2023, Elsevier.

a factor in the enhanced corrosion resistance, demonstrating that increased stability is due to surface complex formation on the Ni group and passivation. Tang *et al.* found that a decrease in pH around the anode during the electrolysis of seawater accelerated the corrosion of the electrode material by chloride ions, and that this corrosion behaviour increased rapidly with increasing current density.[151] The researchers classified the results of electrochemical testing of the materials at different pH and current densities and found that the electrode materials can undergo a stable oxygen precipitation reaction in the blue, low-current-density, high-pH region, while the electrodes dissolve violently in the red, high-current-density, low-pH region (Fig. 15d). This finding draws attention to the fact that, in addition to a corrosion-resistant strategy for the catalyst, the construction of a long-lasting electrolyte/electrolyte interfacial microenvironment is an important factor in determining the stability of electrolytic seawater.[153]

4.3 Doped corrosion-resistant ions

Doping the catalyst with corrosion-resistant ions is another effective method to extend its service life. Incorporating metal ions with good corrosion resistance into the catalyst's structure enhanced its ability to resist corrosion by chloride ions.[154] These corrosion-resistant metal ions not only improve the surface redox activity of the catalyst but also help reduce the corrosive impact of chlorides on the catalyst.[155,156] Ou *et al.* uniformly doped Mo into Ni_3S_2 to obtain Mo–Ni_3S_2/NMF (Fig. 16c). Electrochemical measurements and DFT calculations revealed that Mo doping increased the binding energy with *OH and decreased the binding energy with *Cl on the catalyst surface, thereby enhancing corrosion resistance (Fig. 16a and b).[157] Meanwhile, the *in situ*-grown SO_x^{n-} also improves the corrosion resistance of the catalyst through the principle of electrostatic repulsion, which can maintain the stability of 160 h at 1.53 V. Rare earth elements have good chemical stability and corrosion resistance, and the doping of appropriate amount of rare earth ions in the catalyst can improve its corrosion resistance. Recently, Yao *et al.* doped Ce on NiFe LDH, and Ce generated a protective layer of CeO_2 to prevent chloride ions from penetrating the catalytic layer during the electrolysis of seawater.[83] The electrocatalyst can work stably for 500 h at a current density of 1000 mA cm^{-2}, a finding that points the way to exploring Ce-doped LDH. Multi-component catalysts, such as high-entropy alloys, offer enhanced corrosion resistance through the coordination of each metal component, compared to single mono or binary metal catalysts.[159] Bian *et al.* used a one-step electrodeposition method to construct a high-entropy alloy multi-component catalyst NiFeCuCoCe HEA on a nickel foam substrate. Further, they enhanced the corrosion resistance of the material through the *in situ* growth of various hydroxyl oxides on the surface of the catalyst by modification (Fig. 16d–f).[158] Characterizing the surface of the catalyst after the OER by XPS, the researchers found that there was no significant reconstruction of the surface of the samples used for a long period of time, demonstrating the good corrosion resistance of the catalyst. This is attributed to the incorporation of NiCuCe corrosion-resistant elements and the formation of a dense layered structure on the catalyst surface during modification, both of which work in tandem to prevent the corrosion of chloride ions.

5. Conclusions and outlook

Seawater, as an abundant renewable resource on the planet, provides a high-quality source of direct electrolysis for hydrogen production. This method enables the production of hydrogen and freedom from dependence on other fossil fuels, making it an essential means of contributing to the goal of carbon neutrality by 2060.[160] The process of direct electrolysis of seawater for hydrogen production has the unique advantage of not only avoiding pollutants and greenhouse gases, but also serving as a sustainable source of hydrogen energy. However, the existence of expensive production costs of precious metal catalysts and the challenge of corrosion of catalysts by seawater make direct electrolysis of seawater unattainable for large-scale commercial applications. Facing this background, the research progress for modifying non-precious-metal nickel-based electrolyte materials and the corrosion-resistant strategy of nickel-based catalysts in seawater have attracted much attention in recent years.

This review provides an overview of the subject, summarising the latest research advances and strategies. The principle of seawater electrolysis, the basis for judging electrocatalyst activity, and the pathways reported in recent years to improve the catalytic activity and stability of OER and HER in seawater electrolysis with modified nickel-based electrolyte materials are explained. Meanwhile, effective corrosion resistance strategies in recent years are summarised to study catalyst corrosion in seawater environments. These research results point the way to the further development and commercial application of direct electrolysis of seawater for hydrogen production. By reducing catalyst costs, improving catalytic activity and stability, and designing corrosion-resistant nickel-based catalysts, we are expected to overcome the current technological limitations and promote the large-scale application of direct electrolysis of seawater for hydrogen production, which will make a significant contribution to the achievement of sustainable energy development and the goal of carbon neutrality.

Although nickel-based catalysts have achieved electrochemical activity comparable to commercial noble metal-based catalysts through modification, the current technology is still unable to meet the demand for large-scale commercial applications.[161,162] The main reasons for this status quo are twofold. Firstly, these modified nickel-based catalysts are still in the laboratory stage, with low yields for single synthesis and time-consuming preparation processes, making it impossible to achieve batch production.[163] Secondly, it is important to note that despite the improvements achieved by doping the catalyst with corrosion-resistant ions, there are still challenges in the stability of these modified catalysts during high-current, long-duration seawater-catalyzed electrolysis. Further research is required to address these issues effectively. In the future, efforts can be focused on enhancing the electrochemical performance of nickel-based catalysts to a level where they can be utilized commercially.[164,165]

5.1 Further exploration of corrosion resistance strategies

In the future, to further promote the commercialisation of electrolytic seawater, researchers should continue to gain a deeper understanding of the mechanism of electrolytic seawater as well as propose corrosion-resistant strategies. For example, corrosion-resistant materials and new synthesis pathways can be selected.[35] Materials with good corrosion resistance are sought as growth substrates for electrocatalysts. These materials can include corrosion-resistant metals or alloys and carbon-based materials with excellent corrosion resistance.[166] In addition, modifying and protecting the surface of the electrocatalyst can enhance its corrosion resistance. For example, suitable surface coatings, films or encapsulating materials are used to block corrosive substances in seawater from coming into direct contact with the catalyst. Surface modification can also improve the stability of the electrocatalyst by changing the surface chemistry or forming a protective oxide layer, for example. By optimizing the characteristics of the catalyst in terms of nanostructure as well as crystal morphology, it is also an excellent way to improve its corrosion resistance. For example, reasonable control of the lattice defects and pore structure of the catalyst can enhance its corrosion resistance and improve the catalytic activity. It is worth noting that regulating the environmental conditions of the catalytic reaction, such as controlling the pH value and temperature of the electrolyte, can optimize the corrosion resistance of the electrocatalyst. Appropriate electrolyte composition and concentration are reasonably selected to avoid the corrosion of the catalyst by excessive pH and ion concentration. Finally, advanced monitoring and analysis techniques, such as *in situ* spectroscopy and electrochemical testing, are used to track and evaluate the performance of the electrocatalyst in a corrosive environment in real-time. This will help to understand the corrosion mechanism and provide guidance for optimising the design and regulation of electrocatalysts.

5.2 Developing more efficient and scaleable synthesis methods

Optimization of the synthesis conditions can be carried out to find the best reaction conditions by precisely controlling the synthesis conditions such as reaction temperature, pressure, catalyst concentration, and the amount of additives used. Reasonable synthesis conditions can increase the reaction rate and yield, thus improving the preparation efficiency of nickel-based catalysts.[167] At the same time, through the improvement and optimization of the synthesis route, the intermediate reaction steps and energy consumption can be reduced, and the reaction conversion and catalyst yield can be increased. Process simulation techniques and reaction engineering principles can be used to guide the optimal design of synthetic routes. Some existing novel synthetic methods, such as microfluidic synthesis, sol–gel method, hydrothermal synthesis, *etc.*, can replace the traditional synthetic methods.[163] Further study of these novel synthetic methods can provide higher reaction control and higher reaction rates, thus increasing the yield of nickel-based catalysts.

5.3 Improvement of catalyst stability

To improve the stability of the catalyst, we can adopt a series of strategies. Firstly, choose catalyst support materials reasonably, such as carbon materials with good chemical stability and conductivity, oxides, or stable high surface area materials. Second, enhance the compatibility of the catalyst with the electrolyte through surface modification and functionalisation to reduce the reaction with impurities in seawater and improve the stability of the catalyst.[168] At the same time, the surface structure and composition of the catalyst are optimized to increase the number and activity of active sites, and active site engineering is carried out to improve catalytic activity and stability. In addition, the mass transfer performance and stability of the catalysts are enhanced by designing and optimizing the electrode structure of the catalysts, including morphology, pore structure, and pore size. In addition, the conductivity performance of the catalyst can be improved by doping or modulating the electronic structure of the catalyst.[169] Finally, a suitable electrolyte formulation is selected, and stabilizers, buffers, or additives are added to optimise the electrolyte and improve the stability of the catalyst in seawater. The combined application of these strategies can effectively improve the stability of modified nickel-based catalysts to withstand high currents and prolonged catalytic electrolysis reactions in seawater environments and promote the commercial application of seawater direct electrolysis for hydrogen production technology. This will provide important support for the development of sustainable energy and the achievement of carbon neutrality.

Data availability

The data used to support the review are included within the article.

Conflicts of interest

There are no conflicts to declare.

Acknowledgements

Supports of the National Natural Science Foundation of China (21902021, 21908017), the Fundamental Research Funds for the Central Universities (DUT22LK09), the Open Foundation of Key Laboratory of Industrial Ecology and Environmental Engineering, MOE (KLIEEE-21-02), the Foundation of State Key Laboratory of High-efficiency Utilization of Coal and Green Chemical Engineering (2022-K70), and the Hefei Advanced Computing Center for this work are gratefully acknowledged.

References

1 D. S. Kaufman and E. Broadman, Revisiting the Holocene global temperature conundrum, *Nature*, 2023, **614**, 425–435.
2 T. R. Karl, A. Arguez, B. Y. Huang, J. H. Lawrimore, J. R. McMahon, M. J. Menne, T. C. Peterson, R. S. Vose and H. M. Zhang, Possible artifacts of data biases in the

recent global surface warming hiatus, *Science*, 2015, **348**, 1469–1472.
3 Z. Xie, B. Han, Y. Sun, B. L. Su, J. Yang, X. Bao and M. He, Green carbon science for carbon neutrality, *Natl. Sci. Rev.*, 2023, **10**, nwad225.
4 T. Jiang, X. He, B. Su, P. H. Havea, K. Wei, Z. W. Kundzewicz and D. Liu, COP 28: Challenge of coping with climate crisis, *Innovation*, 2024, **5**, 100559.
5 K. Sanderson, COP28 climate summit signals the end of fossil fuels — but is it enough?, *Nature*, 2023, **624**(7992), 484–485.
6 H. The, Lancet Planetary, COP28 reflections, *Lancet*, 2024, **8**, e1.
7 R. Li, Y. Li, P. Yang, P. Ren, D. Wang, X. Lu, R. Xu, Y. Li, J. Xue, J. Zhang, M. An, J. Ma, B. Wang, H. Liu and S. Dou, Synergistic interface engineering and structural optimization of non-noble metal telluride-nitride electrocatalysts for sustainably overall seawater electrolysis, *Appl. Catal., B*, 2022, **318**, 121834.
8 Y. Li, H. Xu, P. Yang, R. Li, D. Wang, P. Ren, S. Ji, X. Lu, F. Meng, J. Zhang and M. An, Interfacial engineering induced highly efficient CoNiP@NiFe layered double hydroxides bifunctional electrocatalyst for water splitting, *Mater. Today Energy*, 2022, **25**, 100975.
9 R. Li, Y. Li, P. Yang, P. Ren, D. Wang, X. Lu, H. Zhang, Z. Zhang, P. Yan, J. Zhang, M. An, B. Wang, H. Liu and S. Dou, Key Roles of Interfacial OH- ion Distribution on Proton Coupled Electron Transfer Kinetics Toward Urea Oxidation Reaction, *Small*, 2023, **19**, e2302151.
10 R. Li, P. Ren, P. Yang, Y. Li, D. Wang, X. Lu, H. Zhang, F. Meng, X. Peng, B. Yuan, B. Wang, J. Zhang, M. An and G. Wu, VO_x-doped CoP catalysts with synergistic dual-active configuration for boosting hydrogen evolution kinetics, *Nano Energy*, 2024, **126**, 109613.
11 P. Nikolaidis and A. Poullikkas, A comparative overview of hydrogen production processes, *Renewable Sustainable Energy Rev.*, 2017, **67**, 597–611.
12 A. I. Osman, N. Mehta, A. M. Elgarahy, M. Hefny, A. Al-Hinai, A. H. Al-Muhtaseb and D. W. Rooney, Hydrogen production, storage, utilisation and environmental impacts: a review, *Environ. Chem. Lett.*, 2022, **20**, 153–188.
13 H. Yang, M. Driess and P. W. Menezes, Self-Supported Electrocatalysts for Practical Water Electrolysis, *Adv. Energy Mater.*, 2021, **11**, 2102074.
14 W. He, X. Li, C. Tang, S. Zhou, X. Lu, W. Li, X. Li, X. Zeng, P. Dong, Y. Zhang and Q. Zhang, Materials Design and System Innovation for Direct and Indirect Seawater Electrolysis, *ACS Nano*, 2023, **17**, 22227–22239.
15 Q. Fu, J. Han, X. Wang, P. Xu, T. Yao, J. Zhong, W. Zhong, S. Liu, T. Gao, Z. Zhang, L. Xu and B. Song, 2D Transition Metal Dichalcogenides: Design, Modulation, and Challenges in Electrocatalysis, *Adv. Mater.*, 2021, **33**, e1907818.
16 Y. Zheng, Y. Jiao, Y. Zhu, L. H. Li, Y. Han, Y. Chen, M. Jaroniec and S. Z. Qiao, High Electrocatalytic Hydrogen Evolution Activity of an Anomalous Ruthenium Catalyst, *J. Am. Chem. Soc.*, 2016, **138**, 16174–16181.
17 C. Wang, Q. Zhang, B. Yan, B. You, J. Zheng, L. Feng, C. Zhang, S. Jiang, W. Chen and S. He, Facet Engineering of Advanced Electrocatalysts Toward Hydrogen/Oxygen Evolution Reactions, *Nano-Micro Lett.*, 2023, **15**, 52.
18 Y. Wang, M. Wang, Y. Yang, D. Kong, C. Meng, D. Zhang, H. Hu and M. Wu, Potential technology for seawater electrolysis: Anion-exchange membrane water electrolysis, *Chem Catal.*, 2023, **3**, 100643.
19 Z. Y. Yu, Y. Duan, X. Y. Feng, X. Yu, M. R. Gao and S. H. Yu, Clean and Affordable Hydrogen Fuel from Alkaline Water Splitting: Past, Recent Progress, and Future Prospects, *Adv. Mater.*, 2021, **33**, e2007100.
20 A. Badreldin, A. El Ghenymy, A.-R. Al-Zubi, A. Ashour, N. Hassan, A. Prakash, M. Kozusznik, D. V. Esposito, S. U. I. Solim and A. Abdel-Wahab, Stepwise strategies for overcoming limitations of membraneless electrolysis for direct seawater electrolysis, *J. Power Sources*, 2024, **593**, 233991.
21 Y. Dong and S. Komarneni, Strategies to Develop Earth-Abundant Heterogeneous Oxygen Evolution Reaction Catalysts for pH-Neutral or pH-Near-Neutral Electrolytes, *Small Methods*, 2021, **5**, e2000719.
22 M. Maril, J. L. Delplancke, N. Cisternas, P. Tobosque, Y. Maril and C. Carrasco, Critical aspects in the development of anodes for use in seawater electrolysis, *Int. J. Hydrogen Energy*, 2022, **47**, 3532–3549.
23 Z. Xiao, J. Wang, H. Lu, Y. Qian, Q. Zhang, A. Tang and H. Yang, Hierarchical Co/MoNi heterostructure grown on monocrystalline $CoNiMoO_x$ nanorods with robust bifunctionality for hydrazine oxidation-assisted energy-saving hydrogen evolution, *J. Mater. Chem. A*, 2023, **11**, 15749–15759.
24 F. Lu, M. Zhou, Y. Zhou and X. Zeng, First-Row Transition Metal Based Catalysts for the Oxygen Evolution Reaction under Alkaline Conditions: Basic Principles and Recent Advances, *Small*, 2017, **13**, 1701931.
25 N. T. Suen, S. F. Hung, Q. Quan, N. Zhang, Y. J. Xu and H. M. Chen, Electrocatalysis for the oxygen evolution reaction: recent development and future perspectives, *Chem. Soc. Rev.*, 2017, **46**, 337–365.
26 F. Dionigi, T. Reier, Z. Pawolek, M. Gliech and P. Strasser, Design Criteria, Operating Conditions, and Nickel-Iron Hydroxide Catalyst Materials for Selective Seawater Electrolysis, *ChemSusChem*, 2016, **9**, 962–972.
27 X. Ren, X. Dong, Z. Wu, J. Cao, X. Yang, J. Hao, L. Liu, G. Wu and A. Liu, Theoretical study of Au–NX–C catalysts for H2O2 electrosynthesis *via* two-electron oxygen reduction reaction, *Catal. Sci. Technol.*, 2024, **14**, 2226–2234.
28 X. Ren, X. Dong, L. Liu, J. Hao, H. Zhu, A. Liu and G. Wu, Research progress of electrocatalysts for the preparation of H2O2 by electrocatalytic oxygen reduction reaction, *SusMat*, 2023, **3**, 442–470.
29 H. Zhu, X. Ren, X. Yang, X. Liang, A. Liu and G. Wu, Fe-based catalysts for nitrogen reduction toward ammonia electrosynthesis under ambient conditions, *SusMat*, 2022, **2**, 214–242.

30 A. Liu, X. Liang, X. Ren, W. Guan, M. Gao, Y. Yang, Q. Yang, L. Gao, Y. Li and T. Ma, Recent Progress in MXene-Based Materials: Potential High-Performance Electrocatalysts, *Adv. Funct. Mater.*, 2020, **30**, 2003437.
31 J. Guo, Y. Zheng, Z. Hu, C. Zheng, J. Mao, K. Du, M. Jaroniec, S.-Z. Qiao and T. Ling, Direct seawater electrolysis by adjusting the local reaction environment of a catalyst, *Nat. Energy*, 2023, **8**(3), 264–272.
32 Y. Zheng, W. Geng, S. Xiao, T. Ma, C. Cheng, Y. Liao, Z. Zeng, S. Li and C. Zhao, Interfacial Ir-V Direct Metal Bonding Enhanced Hydrogen Evolution Activity in Vanadium Oxides Supported Catalysts, *Angew Chem. Int. Ed. Engl.*, 2024, e202406427.
33 D. Zhang, Y. Shi, J. Yin and J. Lai, Recent Advances for Seawater Hydrogen Evolution, *ChemCatChem*, 2024, e202301305.
34 F. Dingenen and S. W. Verbruggen, Tapping hydrogen fuel from the ocean: A review on photocatalytic, photoelectrochemical and electrolytic splitting of seawater, *Renewable Sustainable Energy Rev.*, 2021, **142**, 110866.
35 J. Dong, C. Yu, H. Wang, L. Chen, H. Huang, Y. Han, Q. Wei and J. Qiu, A robust & weak-nucleophilicity electrocatalyst with an inert response for chlorine ion oxidation in large-current seawater electrolysis, *J. Energy Chem.*, 2024, **90**, 486–495.
36 S. Zhang, Y. Wang, S. Li, Z. Wang, H. Chen, L. Yi, X. Chen, Q. Yang, W. Xu, A. Wang and Z. Lu, Concerning the stability of seawater electrolysis: a corrosion mechanism study of halide on Ni-based anode, *Nat. Commun.*, 2023, **14**, 4822.
37 H. M. Zhang, L. H. Zuo, J. K. Li, S. F. Zhang, J. X. Guo, X. P. Li, G. Liu, P. Wang and J. F. Sun, Research and strategies for efficient electrocatalysts towards anodic oxygen evolution reaction in seawater electrolysis system, *J. Mater. Sci. Technol.*, 2024, **187**, 123–140.
38 X. Kang, F. Yang, Z. Zhang, H. Liu, S. Ge, S. Hu, S. Li, Y. Luo, Q. Yu, Z. Liu, Q. Wang, W. Ren, C. Sun, H. M. Cheng and B. Liu, A corrosion-resistant RuMoNi catalyst for efficient and long-lasting seawater oxidation and anion exchange membrane electrolyzer, *Nat. Commun.*, 2023, **14**, 3607.
39 L. Li, B. Wang, G. W. Zhang, G. Yang, T. Yang, S. Yang and S. C. Yang, Electrochemically Modifying the Electronic Structure of IrO Nanoparticles for Overall Electrochemical Water Splitting with Extensive Adaptability, *Adv. Energy Mater.*, 2020, **10**, 2001600.
40 F. H. Zhang, L. Yu, L. B. Wu, D. Luo and Z. F. Ren, Rational design of oxygen evolution reaction catalysts for seawater electrolysis, *Trends Chem.*, 2021, **3**, 485–498.
41 Z. Zhao, J. P. Sun and X. C. Meng, Recent advances in transition metal-based electrocatalysts for seawater electrolysis, *Int. J. Energy Res.*, 2022, **46**, 17952–17975.
42 M. Abedi, S. Rezaee and S. Shahrokhian, Designing core-shell heterostructure arrays based on snowflake NiCoFe-LTH shelled over W_2N-WC nanowires as an advanced bi-functional electrocatalyst for boosting alkaline water/seawater electrolysis, *J. Colloid Interface Sci.*, 2024, **666**, 307–321.
43 S. J. Liu, S. J. Ren, R. T. Gao, X. H. Liu and L. Wang, Atomically embedded Ag on transition metal hydroxides triggers the lattice oxygen towards sustained seawater electrolysis, *Nano Energy*, 2022, **98**, 107212.
44 B. L. Jiang, J. Y. Li, Y. Y. Cui, S. J. Shi, N. Jiang and J. Guan, Controlled growth of highly active NiMoN(100)-decorated porous N- doped carbon nanotubes on carbon cloth as efficient electrodes for alkaline media and seawater electrolysis, *J. Alloys Compd.*, 2023, **958**, 170371.
45 R. Yang, L. Mei, Z. Lin, Y. Fan, J. Lim, J. Guo, Y. Liu, H. S. Shin, D. Voiry, Q. Lu, J. Li and Z. Zeng, Intercalation in 2D materials and *in situ* studies, *Nat. Rev. Chem*, 2024, **8**, 410–432.
46 L. M. Hong, B. Li, C. D. Jing, Z. H. Zhuang, Y. J. Zhang, H. B. Huang, Q. Q. Jiang and J. G. Tang, Recent advances on cationic vacancy engineering application of oxygen evolution reaction electrocatalyst in seawater, *J. Environ. Chem. Eng.*, 2024, **12**, 111946.
47 Y. Chen, X. Q. Jiang, Y. D. Li, J. Zeng and H. P. Liang, Construction of S-modified Amorphous $Fe(OH)_3$ on NiSe Nanowires as Bifunctional Electrocatalysts for Efficient Seawater Splitting, *ACS Appl. Nano Mater.*, 2024, **7**, 3960–3967.
48 W. Liu, W. Liu, T. Hou, J. Ding, Z. Wang, R. Yin, X. San, L. Feng, J. Luo and X. Liu, Coupling Co-Ni phosphides for energy-saving alkaline seawater splitting, *Nano Res.*, 2024, **17**, 4797–4806.
49 S. Gopalakrishnan, V. Saranya, G. Anandha babu, S. Harish, E. Senthil Kumar and M. Navaneethan, Heterogeneous bimetallic oxysulfide nanostructure (Ni-Co) as hybrid bifunctional electrocatalyst for sustainable overall alkaline simulated seawater splitting, *J. Alloys Compd.*, 2023, **965**, 171124.
50 G. Wang, T. Xiang, X. Ren, L. Zhang and C. Chen, Transition metal-based electrocatalysts for hydrogen production from seawater: A review, *Int. J. Hydrogen Energy*, 2024, **73**, 775–790.
51 F. Zhang, L. Yu, L. Wu, D. Luo and Z. Ren, Rational design of oxygen evolution reaction catalysts for seawater electrolysis, *Trends Chem.*, 2021, **3**, 485–498.
52 H. Saada, B. Fabre, G. Loget and G. Benoit, Is Direct Seawater Splitting Realistic with Conventional Electrolyzer Technologies?, *ACS Energy Lett.*, 2024, 3351–3368.
53 H. Jin, J. Xu, H. Liu, H. Shen, H. Yu, M. Jaroniec, Y. Zheng and S. Z. Qiao, Emerging materials and technologies for electrocatalytic seawater splitting, *Sci. Adv.*, 2023, **9**, eadi7755.
54 H. Sun, Z. Yan, F. Liu, W. Xu, F. Cheng and J. Chen, Self-Supported Transition-Metal-Based Electrocatalysts for Hydrogen and Oxygen Evolution, *Adv. Mater.*, 2020, **32**, e1806326.
55 C. Hu, L. Zhang and J. Gong, Recent progress made in the mechanism comprehension and design of electrocatalysts for alkaline water splitting, *Energy Environ. Sci.*, 2019, **12**, 2620–2645.
56 C. L. Hu, L. Zhang and J. L. Gong, Recent progress made in the mechanism comprehension and design of

electrocatalysts for alkaline water splitting, *Energy Environ. Sci.*, 2019, **12**, 2620–2645.

57 Y. Zheng, Y. Jiao, A. Vasileff and S. Z. Qiao, The Hydrogen Evolution Reaction in Alkaline Solution: From Theory, Single Crystal Models, to Practical Electrocatalysts, *Angew Chem. Int. Ed. Engl.*, 2018, **57**, 7568–7579.

58 D. C. Chen, Z. W. Chen, X. X. Zhang, Z. L. Lu, S. Xiao, B. B. Xiao and C. V. Singh, Exploring single atom catalysts of transition-metal doped phosphorus carbide monolayer for HER: A first-principles study, *J. Energy Chem.*, 2021, **52**, 155–162.

59 A. Parra-Puerto, K. L. Ng, K. Fahy, A. E. Goode, M. P. Ryan and A. Kucernak, Supported Transition Metal Phosphides: Activity Survey for HER, ORR, OER, and Corrosion Resistance in Acid and Alkaline Electrolytes, *ACS Catal.*, 2019, **9**, 11515–11529.

60 W. X. Meng, J. Wang, D. Zhang, J. Xu, F. M. Guo, Y. J. Zhang, R. Pang, A. Y. Cao and Y. Y. Shang, Defective Amorphous Carbon-Coated Carbon Nanotube-Loaded Ruthenium Nanoparticles as Efficient Electrocatalysts for Hydrogen Production, *Small Struct.*, 2023, **4**, 2300098.

61 J. Song, C. Wei, Z. F. Huang, C. Liu, L. Zeng, X. Wang and Z. J. Xu, A review on fundamentals for designing oxygen evolution electrocatalysts, *Chem. Soc. Rev.*, 2020, **49**, 2196–2214.

62 J. S. Yoo, X. Rong, Y. Liu and A. M. Kolpak, Role of Lattice Oxygen Participation in Understanding Trends in the Oxygen Evolution Reaction on Perovskites, *ACS Catal.*, 2018, **8**, 4628–4636.

63 H. Liu, W. Shen, H. Jin, J. Xu, P. Xi, J. Dong, Y. Zheng and S. Z. Qiao, High-Performance Alkaline Seawater Electrolysis with Anomalous Chloride Promoted Oxygen Evolution Reaction, *Angew Chem. Int. Ed. Engl.*, 2023, **62**, e202311674.

64 S. Y. Feng, P. Rao, Y. H. Yu, J. Li, P. L. Deng, Z. Y. Kang, S. L. Wang, Z. P. Miao, Y. J. Shen, X. L. Tian and Z. F. Wu, Self-assembled heterojunction $CoSe_2$@CoO catalysts for efficient seawater electrolysis, *Electrochim. Acta*, 2023, **463**, 142870.

65 Y. Shi and B. Zhang, Correction: Recent advances in transition metal phosphide nanomaterials: synthesis and applications in hydrogen evolution reaction, *Chem. Soc. Rev.*, 2016, **45**, 1781.

66 P. A. Kempler and A. C. Nielander, Reliable reporting of Faradaic efficiencies for electrocatalysis research, *Nat. Commun.*, 2023, **14**, 1158.

67 T. Cui, X. J. Zhai, L. L. Guo, J. Q. Chi, Y. Zhang, J. W. Zhu, X. M. Sun and L. Wang, Controllable synthesis of a self-assembled ultralow Ru, Ni-doped Fe_2O_3 lily as a bifunctional electrocatalyst for large-current-density alkaline seawater electrolysis, *Chin. J. Catal.*, 2022, **43**, 2202–2211.

68 T. Wu, E. Song, S. Zhang, M. Luo, C. Zhao, W. Zhao, J. Liu and F. Huang, Engineering Metallic Heterostructure Based on Ni_3N and 2M-MoS_2 for Alkaline Water Electrolysis with Industry-Compatible Current Density and Stability, *Adv. Mater.*, 2022, **34**, e2108505.

69 W. L. Liang, M. Y. Zhou, X. Y. Lin, J. C. Xu, P. Y. Dong, Z. C. Le, M. Z. Yang, J. Chen, F. Y. Xie, N. Wang, Y. S. Jin and H. Meng, Nickel-doped tungsten oxide promotes stable and efficient hydrogen evolution in seawater, *Appl. Catal., B*, 2023, **325**, 122397.

70 H.-Y. Wang, J.-T. Ren, L. Wang, M.-L. Sun, H.-M. Yang, X.-W. Lv and Z.-Y. Yuan, Synergistically enhanced activity and stability of bifunctional nickel phosphide/sulfide heterointerface electrodes for direct alkaline seawater electrolysis, *J. Energy Chem.*, 2022, **75**, 66–73.

71 A. K. Tareen, G. S. Priyanga, K. Khan, E. Pervaiz, T. Thomas and M. Yang, Nickel-Based Transition Metal Nitride Electrocatalysts for the Oxygen Evolution Reaction, *ChemSusChem*, 2019, **12**, 3941–3954.

72 L. Li, X. Cao, J. Huo, J. Qu, W. Chen, C. Liu, Y. Zhao, H. Liu and G. Wang, High valence metals engineering strategies of Fe/Co/Ni-based catalysts for boosted OER electrocatalysis, *J. Energy Chem.*, 2023, **76**, 195–213.

73 N. Hales, T. J. Schmidt and E. Fabbri, Reversible and irreversible transformations of Ni-based electrocatalysts during the oxygen evolution reaction, *Curr. Opin. Electrochem.*, 2023, **38**, 101231.

74 H. X. Wang, M. Y. Cui, G. L. Fu, J. Y. Zhang, X. Y. Ding, I. Azaceta, M. Bugnet, D. M. Kepaptsoglou, V. K. Lazarov, V. A. D. O'Shea, F. E. Oropeza and K. H. L. Zhang, Vertically aligned Ni/NiO nanocomposites with abundant oxygen deficient hetero-interfaces for enhanced overall water splitting, *Sci. China: Chem.*, 2022, **65**, 1885–1894.

75 H. Khadijeh, A. Kumar, A. R. Jadhav, O. Moradlou, A. Z. Moshfegh and H. Lee, Nanorod Array-Based Hierarchical NiO Microspheres as a Bifunctional Electrocatalyst for a Selective and Corrosion-Resistance Seawater Photo/Electrolysis System, *ACS Catal.*, 2023, **13**, 5516–5528.

76 H. T. Qian, J. Wei, C. C. Yu, F. Tang, W. Jiang, D. S. Xia and L. Gan, In Situ Quantification of the Active Sites, Turnover Frequency, and Stability of Ni-Fe (Oxy)hydroxides for the Oxygen Evolution Reaction, *ACS Catal.*, 2022, **12**, 14280–14289.

77 D. N. Zhang, H. Cheng, X. Y. Hao, Q. Sun, T. Y. Zhang, X. W. Xu, Z. L. Ma, T. Yang, J. Ding, X. Q. Liu, M. Yang and X. L. Huang, Stable Seawater Oxidation at High-Salinity Conditions Promoted by Low Iron-Doped Non-Noble-Metal Electrocatalysts, *ACS Catal.*, 2023, **13**, 15581–15590.

78 C. Debabrata, H. Jaromir, B. Tomas, P. Martin and B. Karel, Optimization of synthesis of the nickel-cobalt oxide based anode electrocatalyst and of the related membrane-electrode assembly for alkaline water electrolysis, *J. Power Sources*, 2017, **347**, 247–258.

79 T. Haq and Y. Haik, NiO_x–FeO_x Nanoclusters Anchored on g-C_3N_4 Sheets for Selective Seawater Oxidation with High Corrosion Resistance, *ACS Sustain. Chem. Eng.*, 2022, **10**, 6622–6632.

80 Z. He, J. Zhang, Z. Gong, H. Lei, D. Zhou, N. Zhang, W. Mai, S. Zhao and Y. Chen, Activating lattice oxygen in NiFe-based

(oxy)hydroxide for water electrolysis, *Nat. Commun.*, 2022, **13**, 2191.
81 Y. Q. Wang, S. Tao, H. Lin, G. P. Wang, K. N. Zhao, R. M. Cai, K. W. Tao, C. X. Zhang, M. Z. Sun, J. Hu, B. L. Huang and S. H. Yang, Atomically targeting NiFe LDH to create multivacancies for OER catalysis with a small organic anchor, *Nano Energy*, 2021, **81**, 105606.
82 M. H. Wang, Z. X. Lou, X. Wu, Y. Liu, J. Y. Zhao, K. Z. Sun, W. X. Li, J. Chen, H. Y. Yuan, M. Zhu, S. Dai, P. F. Liu and H. G. Yang, Operando High-Valence Cr-Modified NiFe Hydroxides for Water Oxidation, *Small*, 2022, **18**, e2200303.
83 Y. C. Yao, S. J. Sun, H. Zhang, Z. X. Li, C. X. Yang, Z. W. Cai, X. He, K. Dong, Y. L. Luo, Y. Wang, Y. C. Ren, Q. Liu, D. D. Zheng, W. H. Zhuang, B. Tang, X. P. Sun and W. C. Hu, Enhancing the stability of NiFe-layered double hydroxide nanosheet array for alkaline seawater oxidation by Ce doping, *J. Energy Chem.*, 2024, **91**, 306–312.
84 H. D. Qi, K. Huang, F. H. K. Pan, R. T. Ma, C. Lian, H. L. Liu and J. Hu, Boosting Direct Seawater Electrolysis through Intercalation Engineering of Layered Double Hydroxides, *Ind. Eng. Chem. Res.*, 2023, **62**, 19674–19682.
85 S. Dresp, T. N. Thanh, M. Klingenhof, S. Brückner, P. Hauke and P. Strasser, Efficient direct seawater electrolysers using selective alkaline NiFe-LDH as OER catalyst in asymmetric electrolyte feeds, *Energy Environ. Sci.*, 2020, **13**, 1725–1729.
86 J. Chen, X. Shi, S. Feng, J. Li, X. Gao, X. Wu, K. Li, A. Qi, C. You and X. Tian, Design of highly active and durable oxygen evolution catalyst with intrinsic chlorine inhibition property for seawater electrolysis, *Nano Mater. Sci.*, 2023, DOI: **10.1016/j.nanoms.2023.10.003**.
87 Z. Zhang, K. Ye, H. Du and X. Li, In situ electrodeposition synthesis of CoP@NiFe LDH heterostructure as high-performance electrocatalyst for enhanced seawater electrolysis, *Int. J. Hydrogen Energy*, 2024, **62**, 722–731.
88 Y. Xia, L. Guo, J. Zhu, J. Tang, Z. Li, X. Liu, J. Chi and L. Wang, Manipulating electronic structure of nickel phosphide *via* asymmetric coordination interaction for anion-exchange membrane based seawater electrolysis, *Appl. Catal., B*, 2024, **351**, 123995.
89 X. Liu, Q. Yu, X. Qu, X. Wang, J. Chi and L. Wang, Manipulating Electron Redistribution in Ni(2) P for Enhanced Alkaline Seawater Electrolysis, *Adv. Mater.*, 2024, **36**, e2307395.
90 Y. Yu, X. Chen, J. Li, Y. Xiao, X. Shi, P. Rao, P. Deng, H. Wen and X. Tian, Ni-based heterostructure with protective phosphide layer to enhance the oxygen evolution reaction for the seawater electrolysis, *Int. J. Hydrogen Energy*, 2024, **51**, 1373–1380.
91 S. J. Lv, Y. Deng, Q. Liu, Z. Q. Fu, X. B. Liu, M. H. Wang, Z. Y. Xiao, B. Li and L. Wang, Carbon-quantum-dots-involved Fe/Co/Ni phosphide open nanotubes for high effective seawater electrocatalytic decomposition, *Appl. Catal., B*, 2023, **326**, 122403.
92 H. Zhao, M. Liu, X. Q. Du and X. S. Zhang, Construction of nickel stannum based sulfide as efficient electrocatalysts for freshwater, seawater and urea oxidation, *Int. J. Hydrogen Energy*, 2024, **58**, 117–127.
93 L. Yu, Q. Zhu, S. Song, B. McElhenny, D. Wang, C. Wu, Z. Qin, J. Bao, Y. Yu, S. Chen and Z. Ren, Non-noble metal-nitride based electrocatalysts for high-performance alkaline seawater electrolysis, *Nat. Commun.*, 2019, **10**, 5106.
94 C. Fu, W. Hao, J. Fan, Q. Zhang, Y. Guo, J. Fan, Z. Chen and G. Li, Fabrication of Ultra-Durable and Flexible NiP(x) -Based Electrode toward High-Efficient Alkaline Seawater Splitting at Industrial Grade Current Density, *Small*, 2023, **19**, e2205689.
95 L. Yang, Y. Zhao, L. Zhu and D. Xia, Rational construction of grille structured P-CoZnO-Cu2SeS/NF composite electrocatalyst for boosting seawater electrolysis and corrosion resistance, *Appl. Surf. Sci.*, 2023, **631**, 157541.
96 Y. Song, X. Zhang, Z. Xiao, Y. Wang, P. Yi, M. Huang and L. Zhang, Coupled amorphous NiFeP/crystalline Ni_3S_2 nanosheets enables accelerated reaction kinetics for high current density seawater electrolysis, *Appl. Catal., B*, 2024, **352**, 124028.
97 S. W. Wu, S. Q. Liu, X. H. Tan, W. Y. Zhang, K. Cadien and Z. Li, Ni_3S_2-embedded NiFe LDH porous nanosheets with abundant heterointerfaces for high-current water electrolysis, *Chem. Eng. J.*, 2022, **442**, 136105.
98 C. Z. Wang, M. Zhu, Z. Cao, P. Zhu, Y. Cao, X. Y. Xu, C. Xu and Z. Y. Yin, Heterogeneous bimetallic sulfides based seawater electrolysis towards stable industrial-level large current density, *Appl. Catal., B*, 2021, **291**, 120071.
99 Y. J. Sun, S. Kang, K. M. Kim, S. Mhin, J. C. Kim, S. J. Kim, E. Enkhtuvshin, S. Choi and H. Han, Sulfur-incorporated nickel-iron layered double hydroxides for effective oxygen evolution reaction in seawater, *Appl. Surf. Sci.*, 2021, **568**, 150965.
100 X. Luo, P. Ji, P. Wang, X. Tan, L. Chen and S. Mu, Spherical Ni_3S_2/Fe-NiPx Magic Cube with Ultrahigh Water/Seawater Oxidation Efficiency, *Adv. Sci.*, 2022, **9**, e2104846.
101 M. A. N. Manar, B. Z. Mohamed, M. E.-B. Haitham, G. M. Gehad and E. E.-K. Mohamed, Two-dimensional nickel cyano-bridged coordination polymer thermally derived potent electrocatalysts for alkaline hydrogen evolution reaction, *J. Mater. Chem. A*, 2023, **11**, 24261–24271.
102 X. Wang, G. Liu, D. Zhang, S. Han, J. Yin, J. Jiang, W. Wang and Z. Li, N-doped carbon sheets supported P-Fe_3O_4-MoO_2 for freshwater and seawater electrolysis, *J. Colloid Interface Sci.*, 2023, **652**, 1217–1227.
103 B. R. Wang, M. J. Lu, D. Chen, Q. Zhang, W. W. Wang, Y. T. Kang, Z. X. Fang, G. S. Pang and S. H. Feng, Ni_xFe_yN@C microsheet arrays on Ni foam as an efficient and durable electrocatalyst for electrolytic splitting of alkaline seawater, *J. Mater. Chem. A*, 2021, **9**, 13562–13569.
104 Y. Q. Zhao, B. Jin, A. Vasileff, Y. Jiao and S. Z. Qiao, Interfacial nickel nitride/sulfide as a bifunctional electrode for highly efficient overall water/seawater electrolysis, *J. Mater. Chem. A*, 2019, **7**, 8117–8121.
105 H. Sun, J. Sun, Y. Song, Y. Zhang, Y. Qiu, M. Sun, X. Tian, C. Li, Z. Lv and L. Zhang, Nickel-Cobalt Hydrogen Phosphate on Nickel Nitride Supported on Nickel Foam

for Alkaline Seawater Electrolysis, *ACS Appl. Mater. Interfaces*, 2022, **14**, 22061–22070.

106 L. Lin, S. Piao, Y. Choi, L. Lyu, H. Hong, D. Kim, J. Lee, W. Zhang and Y. Piao, Nanostructured Transition Metal Nitrides as Emerging Electrocatalysts for Water Electrolysis: Status and Challenges, *EnergyChem*, 2022, **4**, 100072.

107 S. Gopalakrishnan, G. Anandha babu, S. Harish, E. S. Kumar and M. Navaneethan, Interface engineering of heterogeneous NiMn layered double hydroxide/vertically aligned $NiCo_2S_4$ nanosheet as highly efficient hybrid electrocatalyst for overall seawater splitting, *Chemosphere*, 2024, **350**, 141016.

108 J. Zhou, J. Liang, Z. Fan, W. Tan, X. Sun, R. Ding, P. Gao and Y. Zhang, $NiFe_2O_4/Ni_2P$ Mott-Schottky heterojunction boosts the oxygen evolution reaction in alkaline water/natural seawater, *Int. J. Hydrogen Energy*, 2024, **51**, 770–778.

109 Y. Huang, J. R. Han, H. B. Wang, L. H. Liu and H. Y. Liang, Multiple metallic dopants in nickel nanoparticles for electrocatalytic oxygen evolution, *Prog. Nat. Sci.: Mater. Int.*, 2023, **33**, 67–73.

110 D. Wu, D. Chen, J. Zhu and S. Mu, Ultralow Ru Incorporated Amorphous Cobalt-Based Oxides for High-Current-Density Overall Water Splitting in Alkaline and Seawater Media, *Small*, 2021, **17**, e2102777.

111 S. H. Wang, P. Yang, X. F. Sun, H. L. Xing, J. Hu, P. Chen, Z. T. Cui, W. K. Zhu and Z. J. Ma, Synthesis of 3D heterostructure Co-doped Fe_2P electrocatalyst for overall seawater electrolysis, *Appl. Catal., B*, 2021, **297**, 120386.

112 C. Q. Huang, Q. C. Zhou, L. Yu, D. S. Duan, T. Y. Cao, S. H. Qiu, Z. Z. Wang, J. Guo, Y. X. Xie, L. P. Li and Y. Yu, Functional Bimetal Co-Modification for Boosting Large-Current-Density Seawater Electrolysis by Inhibiting Adsorption of Chloride Ions, *Adv. Energy Mater.*, 2023, **13**, 2301475.

113 L. Shao, X. D. Han, L. Shi, T. Z. Wang, Y. S. Zhang, Z. Q. Jiang, Z. X. Yin, X. R. Zheng, J. H. Li, X. P. Han and Y. D. Deng, In Situ Generation of Molybdate-Modulated Nickel-Iron Oxide Electrodes with High Corrosion Resistance for Efficient Seawater Electrolysis, *Adv. Energy Mater.*, 2024, **14**, 2303261.

114 C. Xu, J. Zhao, Z. Zhao, W. Zhang and X. Wang, Surface reconstruction in amorphous CoFe-based hydroxides/crystalline phosphide heterostructure for accelerated saline water electrolysis, *J. Colloid Interface Sci.*, 2024, **659**, 821–832.

115 L. Ji, C. Lv, Z. Chen, Z. Huang and C. Zhang, Nickel-Based (Photo)Electrocatalysts for Hydrogen Production, *Adv. Mater.*, 2018, **30**, e1705653.

116 B. Guo, X. Wen, L. Xu, X. Ren, S. Niu, R. YangCheng, G. Ma, J. Zhang, Y. Guo, P. Xu and S. Li, Noble Metal Phosphides: Robust Electrocatalysts toward Hydrogen Evolution Reaction, *Small Methods*, 2023, e2301469.

117 S. H. Ye, W. Xiong, P. Liao, L. R. Zheng, X. Z. Ren, C. X. He, Q. L. Zhang and J. H. Liu, Removing the barrier to water dissociation on single-atom Pt sites decorated with a CoP mesoporous nanosheet array to achieve improved hydrogen evolution, *J. Mater. Chem. A*, 2020, **8**, 11246–11254.

118 W. L. Yu, Z. Chen, Y. L. Fu, W. P. Xiao, B. Dong, Y. M. Chai, Z. X. Wu and L. Wang, Superb All-pH Hydrogen Evolution Performances Powered by Ultralow Pt-Decorated Hierarchical Ni-Mo Porous Microcolumns, *Adv. Funct. Mater.*, 2023, **33**, 2210855.

119 L. Wang, H. Tao, Y. Liu, Y. Chen, Z. Chen, X. Yang, B. Yang, Z. Li, Q. Dai, C. Lian, L. Lei and Y. Hou, Multiscale modulation of ultra-small ruthenium anchored on bimetallic sulfides for seawater electrolysis at ampere-level current density, *Nano Energy*, 2024, **124**, 109481.

120 X. J. Zhai, Q. P. Yu, G. S. Liu, J. L. Bi, Y. Zhang, J. Q. Chi, J. P. Lai, B. Yang and L. Wang, Hierarchical microsphere MOF arrays with ultralow Ir doping for efficient hydrogen evolution coupled with hydrazine oxidation in seawater, *J. Mater. Chem. A*, 2021, **9**, 27424–27433.

121 H. S. Hu, Z. R. Zhang, Y. W. Zhang, T. Thomas, H. Y. Du, K. K. Huang, J. P. Attfield and M. H. Yang, An ultra-low Pt metal nitride electrocatalyst for sustainable seawater hydrogen production, *Energy Environ. Sci.*, 2023, **16**, 4584–4592.

122 J. Su, Q. Wang, M. Fang, Y. Wang, J. Ke, Q. Shao and J. Lu, Metastable Hexagonal-Phase Nickel with Ultralow Pt Content for an Efficient Alkaline/Seawater Hydrogen Evolution Reaction, *ACS Appl. Mater. Interfaces*, 2023, 51160–51169.

123 J. Na, H. Yu, S. Jia, J. Chi, K. Lv, T. Li, Y. Zhao, Y. Zhao, H. Zhang and Z. Shao, Electrochemical reconstruction of non-noble metal-based heterostructure nanorod arrays electrodes for highly stable anion exchange membrane seawater electrolysis, *J. Energy Chem.*, 2024, **91**, 370–382.

124 J. Jiang, Y. Tian, J. Zhang, C. Zhang and L. Ai, Metallic Cu-incorporated NiFe layered double hydroxide nanosheets enabling energy-saving hydrogen generation from chlorine-free seawater electrolysis coupled with sulfion upcycling, *Fuel*, 2024, **367**, 131506.

125 X. H. Wu, J. S. Qiu and Z. Y. Wang, Rare-Earth Doping Transitional Metal Phosphide for Efficient Hydrogen Evolution in Natural Seawater, *Small Struct.*, 2023, **4**, 2200268.

126 X. Y. Lu, J. Pan, E. Lovell, T. H. Tan, Y. H. Ng and R. Amal, A sea-change: manganese doped nickel/nickel oxide electrocatalysts for hydrogen generation from seawater, *Energy Environ. Sci.*, 2018, **11**, 1898–1910.

127 Z. X. Zhu, L. Luo, Y. X. He, M. Mushtaq, J. Q. Li, H. Yang, Z. Khanam, J. Qu, Z. M. Wang and M. S. Balogun, High-Performance Alkaline Freshwater and Seawater Hydrogen Catalysis by Sword-Head Structured Mo_2N-Ni_3Mo_3N Tunable Interstitial Compound Electrocatalysts, *Adv. Funct. Mater.*, 2023, **34**, 2306061.

128 N. B. Ysea, V. B. Llorente, A. Loiacono, L. L. Marquez, L. Diaz, G. I. Lacconi and E. A. Franceschini, Critical insights from alloys and composites of Ni-based electrocatalysts for HER on NaCl electrolyte, *J. Alloys Compd.*, 2022, **915**, 165352.

129 X. M. Bu, X. Y. Liang, Y. Bu, Q. Quan, Y. Meng, Z. X. Lai, W. Wang, C. T. Liu, J. Lu, C. M. L. C. Wu and J. Ho, NiMo@CN heterostructures with multiple electronic transmission channels for highly efficient hydrogen evolution from alkaline electrolytes and seawater, *Chem. Eng. J.*, 2022, **438**, 135379.

130 Z. H. Ge, B. Fu, J. P. Zhao, X. Li, B. Ma and Y. T. Chen, A review of the electrocatalysts on hydrogen evolution reaction with an emphasis on Fe, Co and Ni-based phosphides, *J. Mater. Sci.*, 2020, **55**, 14081–14104.

131 H. Zhang, Y. L. Wang, B. Zhang, S. L. Zhang, Y. R. Ma, Z. X. Wu, Y. J. Zhu, F. S. Liu, Z. Y. Xiao and L. Wang, Interwoven N-doped carbon nanotubes with capped Ni-doped FeP as double-functional electrocatalysts for overall seawater electrolysis, *Sci. China Mater.*, 2023, **66**, 4630–4638.

132 J. T. Ren, L. Chen, W. W. Tian, X. L. Song, Q. H. Kong, H. Y. Wang and Z. Y. Yuan, Rational Synthesis of Core-Shell-Structured Nickel Sulfide-Based Nanostructures for Efficient Seawater Electrolysis, *Small*, 2023, **19**, e2300194.

133 T. Zhao, S. Wang, C. Jia, C. Rong, Z. Su, K. Dastafkan, Q. Zhang and C. Zhao, Cooperative Boron and Vanadium Doping of Nickel Phosphides for Hydrogen Evolution in Alkaline and Anion Exchange Membrane Water/Seawater Electrolyzers, *Small*, 2023, **19**, e2208076.

134 Y. Zou, M. Jin, D. Zhu and Y. J. Tang, Surface Adsorption of Amorphous Phosphate on RuNi-Doped Molybdate for the Hydrogen Evolution Reaction, *Inorg. Chem.*, 2023, **62**, 15757–15765.

135 W. Xu, T. Ma, H. Chen, D. Pan, Z. Wang, S. Zhang, P. Zhang, S. Bao, Q. Yang, L. Zhou, Z. Tian, S. Dai and Z. Lu, Scalable Fabrication of Cu_2S@NiS@Ni/NiMo Hybrid Cathode for High-Performance Seawater Electrolysis, *Adv. Funct. Mater.*, 2023, **33**, 2302263.

136 J. Fan, X. Ma, J. Xia, L. Zhang, Q. Bi and W. Hao, Corrosion resistance and earth-abundance FeS-based heterojunction catalyst for seawater splitting at industrial grade density, *J. Colloid Interface Sci.*, 2024, **657**, 393–401.

137 H. Jin, X. Wang, C. Tang, A. Vasileff, L. Li, A. Slattery and S. Z. Qiao, Stable and Highly Efficient Hydrogen Evolution from Seawater Enabled by an Unsaturated Nickel Surface Nitride, *Adv. Mater.*, 2021, **33**, e2007508.

138 A. Badreldin, A. Nabeeh, Z. K. Ghouri, J. Abed, N. Wang, Y. Wubulikasimu, K. Youssef, D. Kumar, M. K. Stodolny, K. Elsaid, E. H. Sargent and A. Abdel-Wahab, Early Transition-Metal-Based Binary Oxide/Nitride for Efficient Electrocatalytic Hydrogen Evolution from Saline Water in Different pH Environments, *ACS Appl. Mater. Interfaces*, 2021, **13**, 53702–53716.

139 X. Wang, X. Zhang, Y. Xu, H. Song, X. Min, Z. Tang, C. Pi, J. Li, B. Gao, Y. Zheng, X. Peng, P. K. Chu and K. Huo, Heterojunction Mo-based binary and ternary nitride catalysts with Pt-like activity for the hydrogen evolution reaction, *Chem. Eng. J.*, 2023, **470**, 144370.

140 R. Y. Fan, X. Y. Zhang, N. Yu, F. G. Wang, H. Y. Zhao, X. Liu, Q. X. Lv, D. P. Liu, Y. M. Chai and B. Dong, Rapid "self-healing" behavior induced by chloride anions to renew the Fe-Ni(oxy)hydroxide surface for long-term alkaline seawater electrolysis, *Inorg. Chem. Front.*, 2022, **9**, 4216–4224.

141 J. W. Koster, S. A. Tornoe, N. P. Kobayashi and D. C. Potts, Explicitly controlling electrical current density overpowers the kinetics of the chlorine evolution reaction and increases the hydrogen production during seawater electrolysis, *Int. J. Hydrogen Energy*, 2023, **48**, 4994–5000.

142 H. Tian and J. Ge, High-efficiency direct seawater electrolysis enabled by electrode microenvironment regulation, *Chem Catal.*, 2023, **3**, 100580.

143 H.-M. Zhang and J. Li, Strategies for overcoming seawater adverse effects on cathodic hydrogen evolution reaction electrocatalysts, *Fuel*, 2024, **367**, 131505.

144 X. Zhou, R. F. Taylor, L. Shi, C. Xie, B. Bian and B. E. Logan, Reducing Chloride Ion Permeation during Seawater Electrolysis Using Double-Polyamide Thin-Film Composite Membranes, *Environ. Sci. Technol.*, 2024, **58**, 391–399.

145 P. Li, S. Zhao, Y. Q. Huang, Q. H. Huang, B. J. Xi, X. G. An and S. L. Xiong, Corrosion Resistant Multilayered Electrode Comprising Ni_3N Nanoarray Overcoated with NiFe-Phytate Complex for Boosted Oxygen Evolution in Seawater Electrolysis, *Adv. Energy Mater.*, 2024, **14**, 2303360.

146 B. Zhang, S. Liu, S. Zhang, Y. Cao, H. Wang, C. Han and J. Sun, High Corrosion Resistance of NiFe-Layered Double Hydroxide Catalyst for Stable Seawater Electrolysis Promoted by Phosphate Intercalation, *Small*, 2022, **18**, e2203852.

147 C. C. Li, B. Zhu, Z. X. Liu, J. T. Zhao, R. R. Meng, L. S. Zhang and Z. G. Chen, Polyelectrolyte-based photothermal hydrogel with low evaporation enthalpy for solar-driven salt-tolerant desalination, *Chem. Eng. J.*, 2022, **431**, 134224.

148 Y. C. Li, X. Y. Wu, J. P. Wang, H. X. Wei, S. Y. Zhang, S. L. Zhu, Z. Y. Li, S. L. Wu, H. Jiang and Y. Q. Liang, Sandwich structured Ni_3S_2-MoS_2-Ni_3S_2@Ni foam electrode as a stable bifunctional electrocatalyst for highly sustained overall seawater splitting, *Electrochim. Acta*, 2021, **390**, 138833.

149 X. Lyu and A. Serov, Cutting-edge methods for amplifying the oxygen evolution reaction during seawater electrolysis: a brief synopsis, *Ind. Chem. Mater.*, 2023, **1**, 475–485.

150 T. Ma, W. Xu, B. Li, X. Chen, J. Zhao, S. Wan, K. Jiang, S. Zhang, Z. Wang, Z. Tian, Z. Lu and L. Chen, The Critical Role of Additive Sulfate for Stable Alkaline Seawater Oxidation on Nickel-Based Electrodes, *Angew Chem. Int. Ed. Engl.*, 2021, **60**, 22740–22744.

151 M. Tang, K. Du, R. Yu, H. Shi, P. Wang, Y. Guo, Q. Wei, H. Yin and D. Wang, Microzone-Acidification-Driven Degradation Mechanism of the NiFe-Based Anode in Seawater Electrolysis, *ACS Appl. Mater. Interfaces*, 2024, **16**, 3260–3269.

152 H. Komiya, K. Obata, T. Honma and K. Takanabe, Dynamic stabilization of nickel-based oxygen evolution electrocatalysts in the presence of chloride ions using

a phosphate additive, *J. Mater. Chem. A*, 2024, **12**, 3513–3522.

153 T. T. He, Q. F. Liu, H. F. Fan, Y. Yang, H. T. Wang, S. Z. Zhang, R. X. Che and E. R. Wang, Exploring the effect of ion concentrations on the electrode activity and stability for direct alkaline seawater electrolysis, *Int. J. Hydrogen Energy*, 2023, **48**, 19385–19395.

154 S. A. Patil, A. C. Khot, V. D. Chavan, I. Rabani, D.-k. Kim, J. Jung, H. Im and N. K. Shrestha, Electrostatically robust CoFeOF nanosheet against chloride for green-H_2 production in alkaline seawater electrolysis, *Chem. Eng. J.*, 2024, **480**, 146545.

155 L. J. Yang, D. Lu, L. J. Zhu and D. H. Xia, Construction of Mo doped CoMoCH-Cu_2SeS/NF composite electrocatalyst with high catalytic activity and corrosion resistance in seawater electrolysis: A case study on cleaner energy, *J. Cleaner Prod.*, 2023, **413**, 137462.

156 S. Ge, X. Shen, J. Gao, K. Ma, H. Zhao, R. Fu, C. Feng, Y. Zhao, Q. Jiao and H. Li, Synergy of Mo doping and heterostructures in $FeCo_2S_4$@Mo-NiCo LDH/NF as durable and corrosion-resistance bifunctional electrocatalyst towards seawater electrolysis at industrial current density, *Chem. Eng. J.*, 2024, **485**, 150161.

157 W. Ou, W. Zhang, H. Qin, W. Zhou, Y. Tang and Q. Gao, Enhancing anti-chlorine corrosion of Ni_3S_2 by Mo-doping for mimic seawater electrolysis, *J. Colloid Interface Sci.*, 2024, **655**, 852–862.

158 H. W. Bian, P. Qi, G. W. Xie, X. Liu, D. Zhang and P. Wang, HEA-NiFeCuCoCe/NF through ultra-fast electrochemical self-reconstruction with high catalytic activity and corrosion resistance for seawater electrolysis, *Chem. Eng. J.*, 2023, **477**, 147286.

159 Y. Z. Shi, B. Yang and P. K. Liaw, Corrosion-Resistant High-Entropy Alloys: A Review, *Metals*, 2017, **7**, 43.

160 R. Ortiz-Imedio, D. G. Caglayan, A. Ortiz, H. Heinrichs, M. Robinius, D. Stolten and I. Ortiz, Power-to-Ships: Future electricity and hydrogen demands for shipping on the Atlantic coast of Europe in 2050, *Energy*, 2021, **228**, 120660.

161 D. Y. Li, L. L. Liao, H. Q. Zhou, Y. Zhao, F. M. Cai, J. S. Zeng, F. Liu, H. Wu, D. S. Tang and F. Yu, Highly active non-noble electrocatalyst from Co_2P/Ni_2P nanohybrids for pH-universal hydrogen evolution reaction, *Mater. Today Phys.*, 2021, **16**, 100314.

162 F. Shiokawa, A. Asilah Haji Tajuddin, T. Ohto, Y. Yu, T. Fujita, H. Tanimoto, Z. Xi, S. Jeong and Y. Ito, Durable high-entropy non-noble metal anodes for neutral seawater electrolysis, *Chem. Eng. J.*, 2024, **479**, 147862.

163 N. Wen, Y. Xia, H. Wang, D. Zhang, H. Wang, X. Wang, X. Jiao and D. Chen, Large-Scale Synthesis of Spinel $Ni_xMn_{3-x}O_4$ Solid Solution Immobilized with Iridium Single Atoms for Efficient Alkaline Seawater Electrolysis, *Adv. Sci.*, 2022, **9**, e2200529.

164 Q. Zhou, L. L. Liao, H. Q. Zhou, D. Y. Li, D. S. Tang and F. Yu, Innovative strategies in design of transition metal-based catalysts for large-current-density alkaline water/seawater electrolysis, *Mater. Today Phys.*, 2022, **26**, 100727.

165 Y. X. Zhao, Q. Y. Sun, C. F. Zhang, F. S. Liu, L. Wang and G. R. Xu, Self-supported electrocatalysts for high-current-density water/seawater electrolysis, *J. Alloys Compd.*, 2023, **968**, 172286.

166 A. Mishra, H. Park, F. El-Mellouhi and D. Suk Han, Seawater electrolysis for hydrogen production: Technological advancements and future perspectives, *Fuel*, 2024, **361**, 130636.

167 M. J. Liang, R. Karthick, Q. Wei, J. H. Dai, Z. S. Jiang, X. C. Chen, T. Z. Oo, S. H. Aung and F. M. Chen, The progress and prospect of the solar-driven photoelectrochemical desalination, *Renewable Sustainable Energy Rev.*, 2022, **155**, 111864.

168 S. Zhang, W. Xu, H. Chen, Q. Yang, H. Liu, S. Bao, Z. Tian, E. Slavcheva and Z. Lu, Progress in Anode Stability Improvement for Seawater Electrolysis to Produce Hydrogen, *Adv. Mater.*, 2024, e2311322.

169 W. Zheng, L. Y. S. Lee and K. Y. Wong, Improving the performance stability of direct seawater electrolysis: from catalyst design to electrode engineering, *Nanoscale*, 2021, **13**, 15177–15187.

